INT. J. REMOTE SENSING, 1985, VOL. 6, NO. 8, 1335–1372

Canopy reflectance, photosynthesis and transpiration

P. J. SELLERS

Hydrological Sciences Branch/Code 624, NASA/Goddard Space Flight Center, Greenbelt, Maryland 20771, U.S.A.

(*Received 19 February 1985*)

Abstract. A two-stream approximation model of radiative transfer is used to calculate values of hemispheric canopy reflectance in the visible and near-infrared wavelength intervals. Simple leaf models of photosynthesis and stomatal resistance are integrated over leaf orientation and canopy depth to obtain estimates of canopy photosynthesis and bulk stomatal or canopy resistance. The ratio of near-infrared and visible reflectances is predicted to be a near linear indicator of minimum canopy resistance and photosynthetic capacity but a poor predictor of leaf area index or biomass.

1. Introduction

A number of recent studies have investigated the correlation between the state of a given terrestrial vegetation cover and its spectral reflectance as obtained via field measurements or from remote-sensing platforms. In particular, efforts have concentrated on:

(1) Relating the simple ratio or the normalized difference (the vegetation index) of the reflected visible and near-infrared radiances to leaf area index and/or biomass (see, for example, Asrar *et al.* 1984, Tucker *et al.* 1981, Curran 1980).

(2) Relating the simple ratio (*sic*) or vegetation index to the amount of photosynthetically active radiation (PAR) absorbed by a vegetated surface (see, for example, Asrar *et al.* 1984).

(3) Relating the time-integral of the amount of PAR absorbed by the vegetation canopy to biomass production (see, for example, Monteith 1977).

This paper explores means by which the simple ratio of the reflectances or the vegetation index may be used to obtain estimates of gross primary productivity and the canopy resistance to transpiration loss. The methods involve the use of models that integrate existing formulations which describe the interception of radiation, photosynthesis and transpiration by individual leaves over whole canopies. Some simplifying assumptions are made to facilitate the solution of the relevant equations, but it is thought that the effect of these simplifications upon the results is small.

The discussion that follows is divided into three parts. The first part describes a radiative transfer model which may be used to calculate the spectral reflectance of vegetated surfaces. Next, mathematical representations of the photosynthetic and transpiration rates of individual leaves as functions of environmental variables are briefly reviewed. Simplified versions of two of these formulae are then integrated in order to calculate values of the photosynthetic rate and the surface resistance of whole

canopies. Lastly, the integrals of photosynthesis and canopy resistance are compared with equivalent simple ratio and vegetation index values.

2. Radiative transfer in vegetative canopies

2.1. *The two-stream approximation radiative transfer model*

Rigorous, realistic models of the interception, scattering and absorption of radiation by vegetation communities have been designed and tested, (see, for example, the work of Suits (1972), Kimes (1984) and Goudriaan (1977). These models describe the process of radiative transfer via a finite-element approach whereby the scattered rays of radiation are traced numerically. Although these techniques allow one to include intricate details regarding the optical characteristics of leaf elements (e.g. non-isotropic scattering), they tend to be computationally expensive and cumbersome to use. The requirement for this investigation is a computationally cheap model that is readily manipulable.

For the purpose of this preliminary study, therefore, we shall use a simple but reasonably realistic analytical approach. Dickinson (1983) reviewed the work of Meador and Weaver (1980) in which the application of the two-stream approximation method to the description of radiative transfer in atmospheres was summarized. The same equations may be adapted to describe radiative transfer in vegetative canopies for which Dickinson (1983) proposed the following form

$$-\bar{\mu}(dI\uparrow/dL)+[1-(1-\beta)\omega]I\uparrow-\omega\beta I\downarrow=\omega\bar{\mu}K\beta_0\exp(-KL) \quad (1)$$

$$\bar{\mu}(dI\downarrow/dL)+[1-(1-\beta)\omega]I\downarrow-\omega\beta I\uparrow=\omega\bar{\mu}K(1-\beta_0)\exp(-KL) \quad (2)$$

where $I\uparrow$ and $I\downarrow$ are the upward and downward diffuse radiative fluxes, normalized by the incident flux, μ is the cosine of the zenith angle of the incident beam, K is the optical depth of direct beam per unit leaf area and is equal to $G(\mu)/\mu$, $G(\mu)$ is the relative projected area of leaf elements in the direction $\cos^{-1}\mu$, $\bar{\mu}$ is the average inverse diffuse optical depth per unit leaf area and is equal to $\int_0^1[\mu'/G(\mu')]\,d\mu'$, μ' is the direction of scattered flux, ω is the scattering coefficient and is equal to $\alpha+\tau$, α is the leaf-element reflectance, τ is the leaf-element transmittance and L is the cumulative leaf area index.

In equations (1) and (2) the individual leaves are treated as isotropic scattering elements. In nature, however, leaf reflectivity commonly increases as the angle between the incident beam and leaf plane decreases. This effect is probably only significant within a narrow range of glancing angles and will be ignored here.

Physical processes can be attributed to each of the four terms in (1) and (2). Equation (1) describes the vertical profile of the upward diffuse radiative flux, $I\uparrow$, within the canopy. It should be noted that both the upward and downward diffuse fluxes are assumed to be completely isotropic. The first term in equation (1) describes the attenuation of the upward diffuse flux. The second term defines that fraction of $I\uparrow$ that is rescattered in an upward direction following interaction with leaf elements. The third terms refers to the fraction of the downward diffuse flux, $I\downarrow$, which is converted into an upward diffuse flux by backscattering. The last term on the righthand side of equation (1) refers to the contribution to the upward diffuse flux by the scattering of direct incident flux penetrating to the specified depth L in the canopy. Corresponding descriptions may be assigned to the four terms in equation (2) which describes the profile of the downward diffuse flux.

β and β_0 are the upscatter parameters for the diffuse and direct beams, respectively.

$\omega\beta$ may be inferred from the analysis of Norman and Jarvis (1975)

$$\omega\beta = \tfrac{1}{2}[\alpha + \tau + (\alpha - \tau)\cos^2\bar{\theta}] \tag{3}$$

$\bar{\theta}$ is the mean leaf inclination angle relative to the horizontal plane (identical to angle between leaf normal and local vertical).

In equation (3) the leaf is treated as an inclined plane with isotropic forward and backscattering properties. A flat leaf ($\cos\bar{\theta} = 1$) will reflect downward fluxes into the upwards direction only and will transmit in the downwards direction only. As the leaf-angle inclination increases, a greater fraction of the downward diffuse flux may be reflected into the lower hemisphere and transmitted into the upper hemisphere.

If equations (1) and (2) are solved in the $\omega \rightarrow 0$ limit (single scatter approximation and semi-infinite canopy), the upward diffuse flux at the canopy top may be taken as equal to the single scattering albedo. Manipulation of the resultant expression gives us an equation for the diffuse upscatter parameter, β_0, where

$$\beta_0 = \frac{1 + \bar{\mu}K}{\omega\bar{\mu}K} a_s(\mu) \tag{4}$$

and $a_s(\mu)$, the single scattering albedo, is given by

$$a_s(\mu) = \omega \int_0^1 \frac{\mu'\Gamma(\mu, \mu')}{[\mu G(\mu') + \mu' G(\mu)]} d\mu' \tag{5}$$

where $\Gamma(\mu, \mu') = G(\mu)G(\mu')P(\mu, \mu')$ and $P(\mu, \mu')$ is the scattering phase function. Much of the above discussion borrows heavily from the review of Dickinson (1983) where a full description of the derivation of the parameters β, β_0 and $a_s(\mu)$ may be found.

A simple expression for $a_s(\mu)$ may be found if we assume isotropic scattering for the leaf elements

$$P(\mu, \mu') \propto 1/G(\mu') \tag{6}$$

The scattering phase function $P(\mu, \mu')$ is now independent of the angle of the incident beam. To satisfy the normalization expression

$$\int_{-1}^{1} P(\mu, \mu')G(\mu')\, d\mu' = 1 \tag{7}$$

$P(\mu, \mu')$ must be equal to $[2G(\mu')]^{-1}$. Insertion of equation (7) into equation (5) yields an expression for $a_s(\mu)$ that may be readily solved for a number of leaf-angle distributions.

Dickinson (1983) adapted a solution from Meador and Weaver (1980) which describes the albedo of a semi-infinite medium. Accordingly the hemispheric canopy albedo, $a_c(\mu)$, for an infinitely thick canopy is defined as

$$\left.\begin{aligned} a_c(\mu) &= I\uparrow \qquad \text{at } L = 0. \\ a_c(\mu) &= \frac{\omega\bar{\mu}K[1 + (2\beta_0 - 1)\beta_1]}{(\beta_2 + \bar{\mu}K)(1 + \beta_1)} \qquad \text{for } L_T \rightarrow \infty \end{aligned}\right\} \tag{8}$$

where L_T is the total leaf area index, $\beta_1 = (1 - \omega)/\beta_2$ and $\beta_2 = (1 - \omega)^{1/2}(1 = \omega + 2\beta\omega)^{1/2}$. Equation (8) provides us with a useful check at one of the limits of the following analysis, i.e. a very dense canopy.

When considering cases where the soil surface may play a part in the scattering of

direct beam radiation (i.e. a sparse canopy), we may solve equations (1) and (2) with boundary conditions appropriate to a vegetative canopy covering a reflective soil surface

$$\left.\begin{aligned} I\downarrow &= 0 \qquad \text{at } L=0 \\ I\uparrow &= \rho_s[I\downarrow + \exp(-KL_T)] \qquad \text{at } L=L_T \end{aligned}\right\} \tag{9}$$

ρ_s is the soil reflectance. The second boundary condition implies that both the downcoming diffuse and direct radiation above the soil surface are reflected isotropically.

The solution of equations (1) and (2) with equation (9) yields

$$\left.\begin{aligned} I\uparrow &= [h_1 \exp(-KL)]/\sigma + h_2 \exp(-hL) + h_3 \exp(hL) \\ I\downarrow &= [h_4 \exp(-KL)]/\sigma + h_5 \exp(-hL) + h_6 \exp(hL) \end{aligned}\right\} \tag{10}$$

The values of the constants, σ, h and h_1 to h_6 are determined from manipulation of equations (1) and (2) and are provided in the Appendix.

The canopy albedo is then simply given by

$$a_c(\mu) = I\uparrow(0) = h_1/\sigma + h_2 + h_3 \tag{11}$$

Suitable boundary conditions may be used in place of equation (9) and the direct radiation terms on the right-hand sides of equations (1) and (2) dropped from the basic equation set to solve for incident diffuse radiative fluxes (see the Appendix). Henceforth, the term albedo will refer to the sum of the diffuse and direct components of albedo.

The exact value of the calculated albedo will depend upon the value of the constants in equation (11) which in turn depend upon

(1) the scattering coefficients for the leaves and soil,
(2) the leaf-area index,
(3) the leaf-angle distribution and
(4) the angle of the incident radiation.

2.2. *Comparison of radiative transfer model results with observations*

Much of the discussion in this paper makes use of optical property values typical of a maize canopy (see, for example, Goudriaan 1977, Dickinson 1983, Miller 1972) as shown in table 1. The following assumptions are made throughout the analysis:

(1) The leaves are randomly arranged in space.
(2) When a mixture of green and dead leaves is specified, they are evenly distributed throughout the canopy.
(3) When a cover fraction is specified, all the vegetation is randomly distributed inside that fraction, the remaining area being completely bare. It is assumed that the length scale of such bare areas is large in relation to the size of individual plants. The total albedo of such an area is then taken as the weighted sum of the albedos of the vegetated and bare areas.

The calculation of hemispheric albedos from equation (11) necessitates the specification of $a_s(\mu)$ for a given leaf-angle distribution from (5). Derivation of the expressions for $a_s(\mu)$ for flat, spherically arranged and vertical leaves is reasonably straightforward and the solutions are listed in table 2. Less regular leaf-angle distributions may be described by means of the χ_L function of Ross (1975) whereby the

Table 1. Optical and physiological properties of maize leaves.

Live leaves	Scattering coefficient	Reflectance	Transmittance
	Leaf optical properties†		
Live leaves			
Visible	0·175	0·105	0·070
Near infrared	0·825	0·577	0·248
Dead leaves			
Visible	0·580	0·360	0·220
Near infrared	0·952	0·577	0·375
	Leaf physiological parameters‡		
a_1 (mg CO_2 dm^{-1} $hour^{-1}$)	82·6	b_1 (W m^{-2})	278·4
a_2 (J m^{-3})	8750	b_2 (W m^{-2})	6 c_2 (s m^{-1}) 55
	Soil optical parameters§		
Visible	0·15		
Near infrared	0·30		

† Dickinson (1983) and Miller (1972).

‡Coefficients from curve fit to data of Hesketh and Baker (1967) and Turner (1974).

The optical properties are averaged values for the wavelength intervals 0·4–0·7 μm (visible) and 0·7–3·0 μm (near infrared). Except where otherwise stated, these values are used throughout the analysis in this paper. (N.B. Equation (15) in text represents a simplification of a model developed to describe C_3 photosynthesis. Here, it has been fitted directly to data to represent the functioning of a C_4 plant, maize, in the absence of an equivalent model.)

§ Optical properties of soil used for this study.

Table 2. Single scattering albedo $a_s(\mu)$ for different leaf-angle distributions. ω is the scattering coefficient and μ is the cosine of solar zenith angle.

Horizontal leaves

$$a_s(\mu)=\omega/4$$

Spherically distributed leaves

$$a_s(\mu)=\frac{\omega}{2}\left[1-\mu\ln\left(\frac{\mu+1}{\mu}\right)\right]$$

Vertical leaves

$$a_s(\mu)=\frac{\psi\omega}{1+\psi^2}\left(\frac{\psi+1}{2}+\frac{\psi}{2\sqrt{(1+\psi^2)}}J\right)$$

$$J=+\ln\left[\frac{\sqrt{(1+\psi^2)}+\psi-x}{\sqrt{(1+\psi^2)}+\psi+x}\right]_{x=0}^{x=1} \qquad x<\sqrt{(1+\psi^2)}$$

$$J=-\ln\left[\frac{x-\psi-\sqrt{(1+\psi^2)}}{x-\psi+\sqrt{(1+\psi^2)}}\right]_{x=0}^{x=1} \qquad x>\sqrt{(1+\psi^2)}$$

$$\psi=\frac{(1-\mu^2)^{1/2}}{\mu}$$

Ross–Goudriaan function: $G(\mu)=\phi_1+\phi_2\mu$

$$a_s(\mu)=\frac{\omega}{2}\frac{G(\mu)}{G(\mu)+\mu\phi_2}\left(1-\frac{\mu\phi_1}{G(\mu)+\mu\phi_2}\ln\left\{\frac{G(\mu)+\mu\phi_1+\mu\phi_2}{\mu\phi_1}\right\}\right)$$

departure of leaf angles from a spherical distribution is characterized by a simple expression

$$\chi_L = \pm \int_0^{\pi/2} |1 - O(\theta)| \sin\theta \, d\theta \tag{12}$$

where θ is the leaf inclination angle relative to the horizontal plane, $O(\theta)$ is the leaf-angle distribution function and $\chi_L = 0$ for spherically arranged leaves, $+1$ for horizontal leaves and -1 for vertical leaves.

Goudriaan (1977) fitted a curve to data sets generated from equation (12) which provides reasonable estimates of the average leaf projection in any direction given the value of χ_L

$$G(\mu) = \phi_1 + \phi_2 \mu \tag{13}$$

where $\phi_1 = 0{\cdot}5 - 0{\cdot}633\chi_L - 0{\cdot}33\chi_L^2$ and $\phi_2 = 0{\cdot}877(1 - 2\phi_1)$. The value of $G(\mu)$ given by equation (13) may be used to obtain values of $a_s(\mu)$ over the range $-0{\cdot}4 < \chi_L < 0{\cdot}6$ (see table 2).

Figure 1 shows calculated global albedo values for a young wheat crop on a clear day in F.R. Germany compared with two days of data obtained from Van der Ploeg *et al.* (1980). For this trial, the data of Dickinson (1983) and Goudriaan (1977) were used to specify the values of the leaf transmittances and reflectances for the visible ($<0{\cdot}7\,\mu$m) and near-infrared ($>0{\cdot}7\,\mu$m) wavelength intervals (see table 1). The incident solar radiation was split into visible and near-infrared direct and diffuse components according to the scheme of Goudriaan (1977, figure 1, page 11). Both the

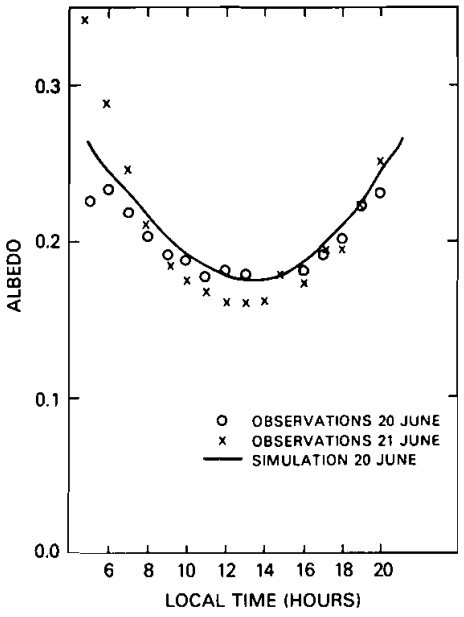

Figure 1. Measured and simulated albedo values for short-wave radiation above a wheat crop. The data points were calculated from observations of incoming and outgoing short wave radiation taken at Volkenrude, F.R. Germany, 20–21 June 1979 (see Van der Ploeg *et al.* 1980). The simulation for the wheat crop at Ruthe (50 km away) for 20 June is also shown.

magnitude of the global albedo (obtained by summing diffuse and direct components of the visible and near-infrared reflectances) and its diurnal variation agree closely with the data. To validate the description of the transmission of radiation through a vegetation canopy, data from another source were used. Fuchs *et al.* (1983) measured diffuse and direct fluxes of photosynthetically active radiation (PAR), taken here to be equivalent to visible radiation, above and below a young wheat canopy (leaf-area index = 1·4). Figure 2 shows the canopy transmittance values as functions of the fraction of direct PAR to total PAR. Also plotted are the predicted transmittances as calculated from the solution of equations (1) and (2). It can be seen that a small error in estimating the *local* leaf-area density (which would result from a slight bias in the positioning of

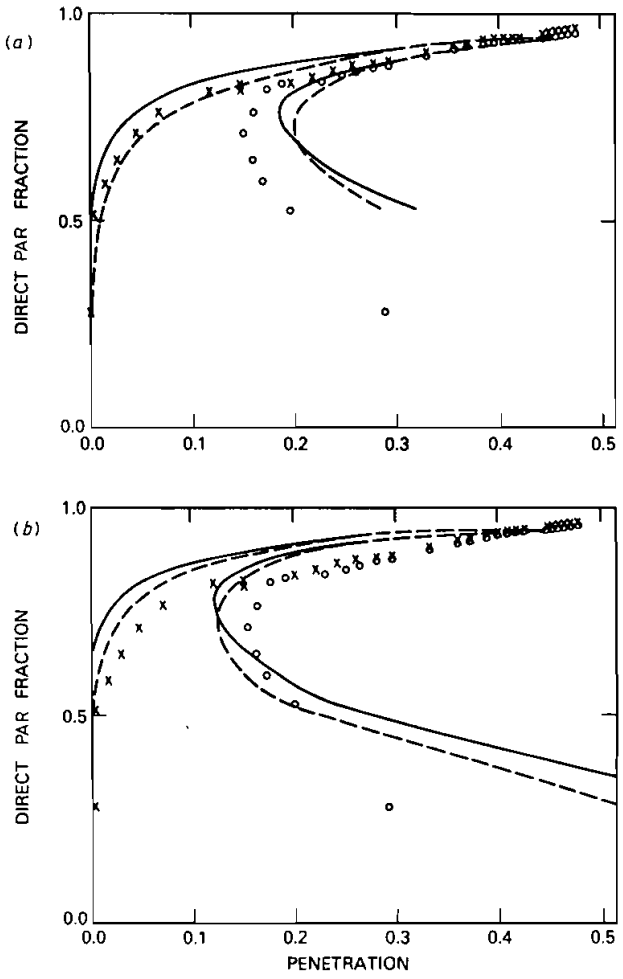

Figure 2. Direct and total transmittances for PAR in a wheat canopy as related to the fraction of direct incident PAR. × and ○ are observations from Fuchs *et al.* (1983) of direct and total PAR penetration, respectively. Solid and dotted lines are predicted values of PAR penetration for inclined (60°) and spherically distributed leaves, respectively. (*a*) Leaf-area index = 1·4 (in accordance with reported value), (*b*) leaf-area index = 1·8; consistent with slight biasing of sensor positions under crop rows. Direct PAR fraction increases with solar elevation; a value of 0·6 corresponds to solar elevation of 10°.

the radiation sensors below the canopy) would result in a large difference in the predicted transmittance at low solar angles. In this case, direct PAR fraction values below 0·6 correspond to solar evaluation angles of $< 10°$. For the higher values of solar elevation, that is PAR fraction $> 0{\cdot}6$, the match between prediction and observation is reasonably good.

Figure 3 shows the predicted absorption of PAR compared with observations from Asrar *et al.* (1984) for a wheat cover over a range of leaf-area-index values. It is clear that a near maximum absorption value of PAR is achieved at a relatively low leaf-area index, somewhere in the range of 2–3. Also, the effect of solar angle on the calculated range of PAR absorption seems to cover the spread of observations, leading one to suspect that this may be one of the main causes of the variation in the data.

Figure 4 shows the predicted variation in surface spectral albedo with the wavelength of incident radiation for a range of leaf-area indices. Soil reflectance is predicted to have only a small effect on albedo in the PAR wavelength interval except when the vegetation cover is very light (the semi-infinite value of albedo is approached when the leaf-area index is only 2). Conversely, the relatively large value of the scattering coefficient of green leaves in the near-infrared region ($\sim 0{\cdot}8$) is predicted to make the effect of soil reflectance on the surface near-infrared albedo significant at higher values of the leaf-area index.

The model may be used to calculate the simple ratio and vegetation index by:

$$\left.\begin{aligned} \text{simple ratio} &= a_{c_{NIR}}/a_{c_{VIS}} \\ \text{vegetation index} &= \frac{a_{c_{NIR}} - a_{c_{VIS}}}{a_{c_{NIR}} + a_{c_{VIS}}} \end{aligned}\right\} \tag{14}$$

where $a_{c_{NIR}}$ is the hemispherically integrated albedo for near-infrared radiation (0·7–3·0 μm) and $a_{c_{VIS}}$ is as above for visible radiation (0·4–0·7 μm).

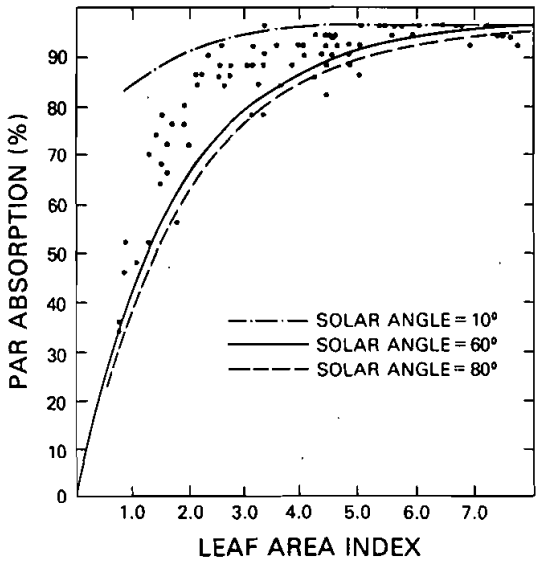

Figure 3. Observed (solid circles) and predicted (lines) absorption of PAR for a growing wheat canopy. Observations are from Asrar *et al.* (1984); predictions are from calculations in the text. Results are for the direct beam radiation only.

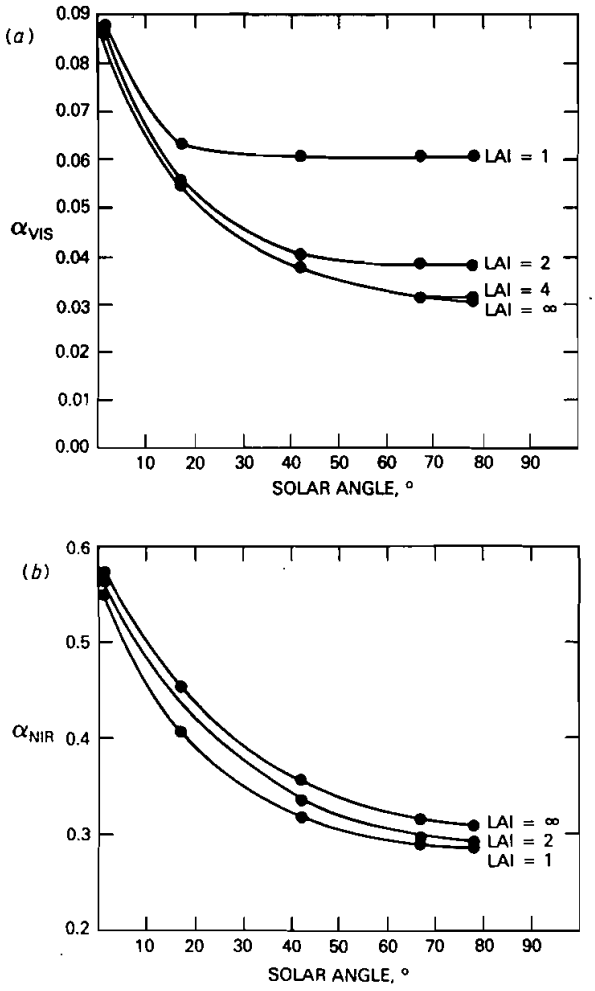

Figure 4. Variation of the albedos of green vegetated surfaces with solar elevation as given by solutions to equations (1) and (2) in the text. (*a*) Albedo for visible wavelength interval, α_{VIS}; $\alpha = 0{\cdot}105$, $\delta = 0{\cdot}007$, $\rho_s = 0{\cdot}15$, (*b*) Albedo for near-infrared wavelength interval, α_{NIR}; $\alpha = 0{\cdot}58$, $\delta = 0{\cdot}25$, $\rho_s = 0{\cdot}30$. (Leaves are distributed spherically and only direct beam radiation considered.)

When comparing these derived values with measurements, it should be noted that the calculated values are hemispherical integrals and that most vegetation index measurements make use of observed unidirectional radiances. Also, the observed albedos are weighted by the relative proportions of downcoming visible and near-infrared radiation. The derived values of the vegetation index compare reasonably well with data (see figure 5) and approach the values derived from the semi-infinite canopy albedos of equation (8) at high leaf-area indices (see figure 4).

Figure 6 shows the calculated variation of the vegetation index with leaf-area index for horizontal leaves with a range of canopy greenness fractions. The results indicate that the presence of any significant fraction of dead material (and presumably material with no chlorophyll—twigs, branches, etc.) severely affects the relationship between

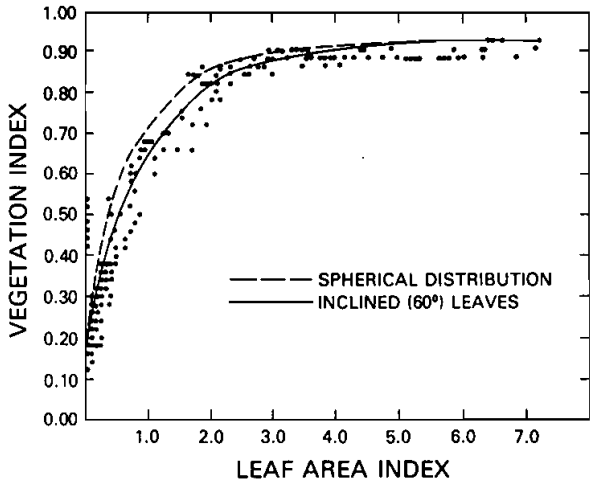

Figure 5. Observed and predicted values of the vegetation index for a growing wheat canopy. Predicted values (lines) are obtained from equation (14) in text; observations (solid circles) are from Asrar *et al.* (1984). N.B. Asrar *et al.* (1984) used narrow band instruments which were presumably nadir viewing: visible interval = 0·6–0·7 μm, near infrared = 0·8–1·1 μm; calculations used leaf optical properties taken from data of Asrar *et al.* (1984) for these wavelength intervals.

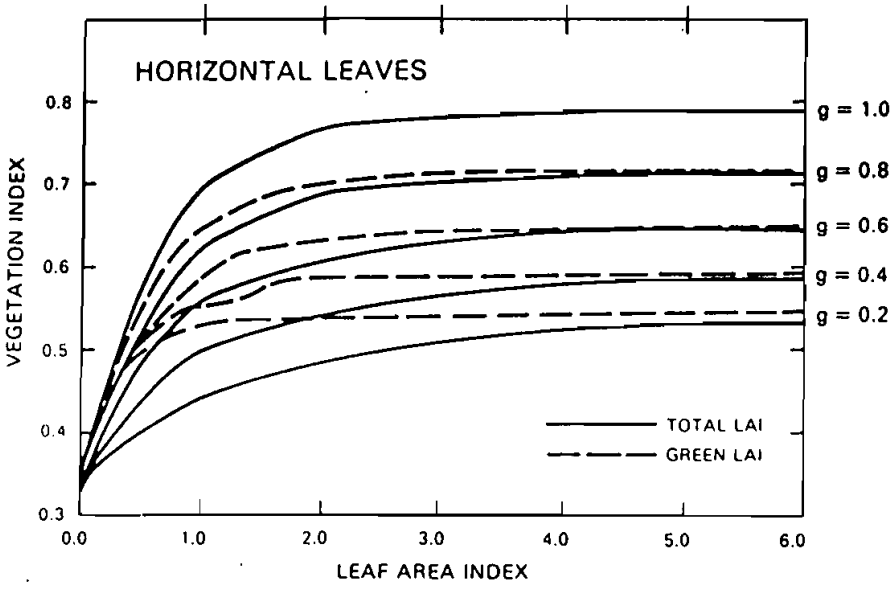

Figure 6. Calculated values of the vegetation index as a function of leaf-area index and canopy greenness (denoted by 'g') for horizontal leaves. The vegetation index is given as a function of total and green leaf area index. Optical properties (broadband) listed in table 1 were used for these calculations.

vegetation index and leaf area index. This finding holds whether one considers total (dead plus live leaves) or just green leaf area index.

The effect of leaf angle and solar elevation on the calculated vegetation index is shown in figure 7. At extreme solar elevations and for low values of the leaf-area index, leaf angle may cause a wide spread in the vegetation index response. The effect is most extreme for vertical leaves which present a maximum optical thickness relative to the direct beam at low solar angles and a zero value for an overhead sun. Horizontal leaves, on the other hand, show no change in vegetation index with solar angle as the optical thickness is invariant with the direction of incident radiation ($G(\mu)/\mu = 1$). With a higher leaf area index, the differences in the response of the vegetation index diminish as the trapping of radiation by the canopy saturates the effect of soil reflectance.

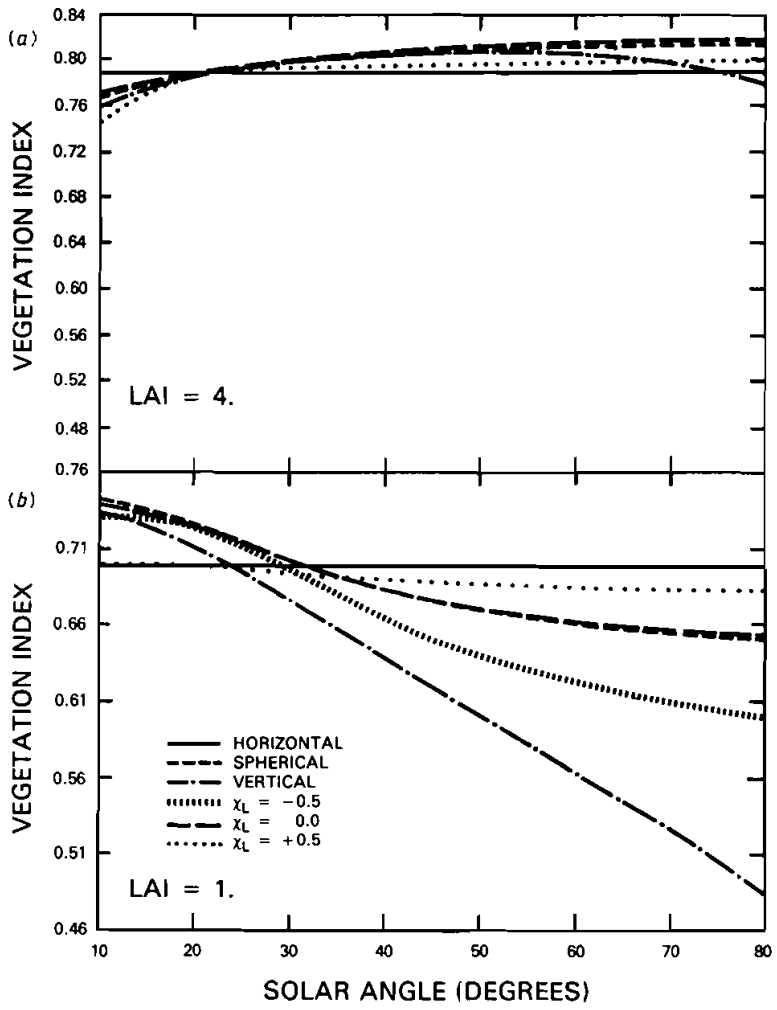

Figure 7. Calculated variation of the vegetation index with solar elevation and leaf-angle distribution for two (1·0 and 4·0) leaf area indices. The interaction of solar elevation and leaf-angle distribution is predicted to have a large effect at low leaf area indices. Optical properties taken from table 1.

Figure 7 also provides us with an indication of the efficacy of the empirical χ_L relationship. The plot for the lower value of leaf area index demonstrates that the response of the spherically distributed leaves and its χ_L analogue ($\chi_L = 0{\cdot}0$) are almost identical. Similarly, the planophile canopy ($\chi_L = +0{\cdot}5$) yields a reasonably close match to the response of the horizontal leaves. The erectophile canopy ($\chi_L = -0{\cdot}5$) shows a similar trend to the variation predicted for vertical leaves but does not attain the same extreme value for high solar elevations. (It must be remembered that the non-zero χ_L factors do not represent canopies with completely horizontal or completely vertical leaves but intermediate distributions approaching one or other extreme.) Generally speaking, the variation described by the χ_L function seems to be in accordance with the trends implied by the 'exact' analytical solutions for vertical, horizontal and spherically distributed leaves.

The question of ambiguous interpretation of the vegetation index arises again when considering the effects of cover fraction. Figure 8 shows the relation between vegetation index and leaf area index where the same amount of area-averaged green-leaf biomass is confined to smaller fractions of the ground area. The presence of only 25 per cent bare ground ($c = 0{\cdot}75$) greatly affects the response. The reason for this is clear; even when the response may be saturated in most of the area, the contribution of the bare ground fraction to the vegetation index is disproportionately strong due to the non-linearity of the vegetation-index/leaf-area-index relationship.

Lastly figure 9 shows data of Asrar *et al.* (1984) relating the vegetation index to the absorbed fraction of PAR. Again, the simulations yield a reasonable agreement with the data and support the proposition that the vegetation index is a near-linear predictor of absorbed PAR.

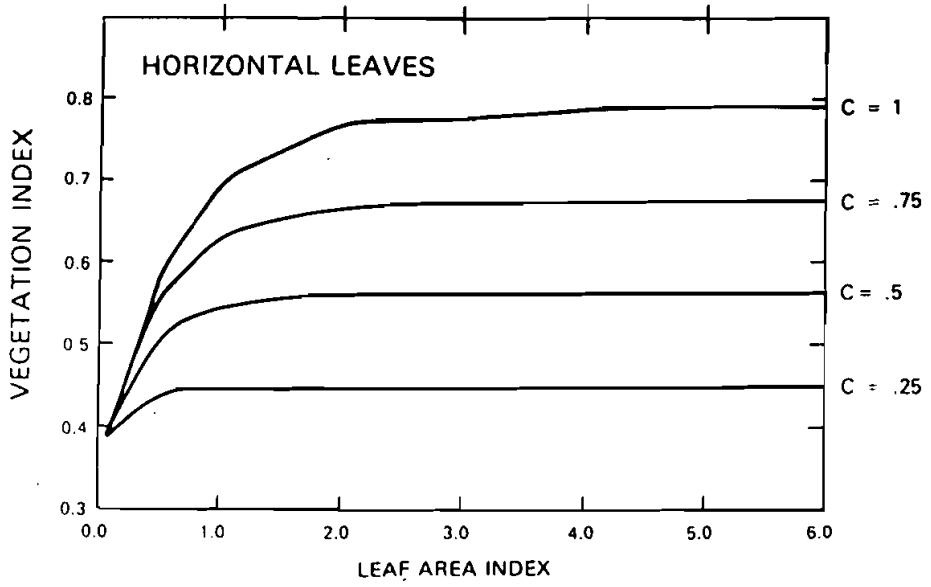

Figure 8. Calculated relation between vegetation index and vegetation cover fraction (denoted by 'c') for horizontal leaves.

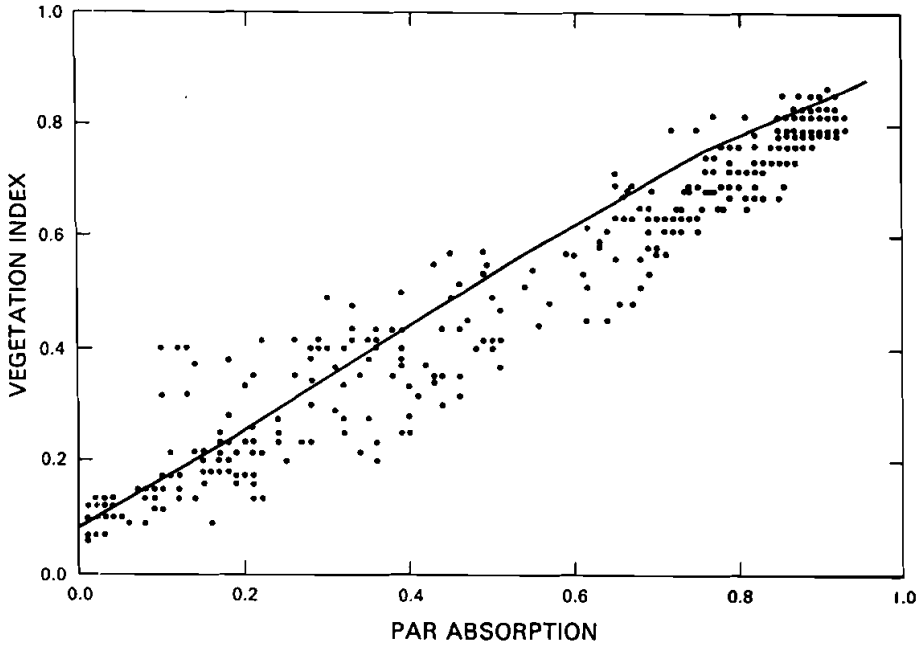

Figure 9. Observed (from Asrar *et al.* 1984) and simulated relationships between vegetation index and absorbed PAR. Spectral properties of leaves and soil were taken to be the same as in figure 5. Solar elevation = 30°, leaves spherically distributed, all radiation direct for simulation.

2.3. *Summary of radiative transfer model results*

The results of the simulations concur with available observations indicating that the model is an adequate tool for this investigation. On the practical side, the results suggest that the vegetation index (plots with the simple ratio show qualitatively similar trends) is an insensitive measure of the leaf area index and/or biomass when either

(1) the leaf-area index exceeds 2 or 3, or
(2) there are patches of bare ground in the sensor field of view, or
(3) there is an unknown quantity of dead material in the canopy, or
(4) the leaf-angle distribution is unknown and the solar elevation is high.

With regard to the last point, effective remote sensing requires strong radiances and is therefore favoured by higher solar elevations.

The next section discusses the relationships between photosynthetic rates and stomatal resistance of individual leaves and vegetative canopies.

3. Photosynthesis and stomatal resistance

3.1. *Leaf photosynthesis*

The biochemistry of photosynthesis and respiration is being actively studied by a number of research groups world-wide and so there is a wide choice of available models. These range from the detailed and elegant descriptions of Farquhar *et al.* (1980), Farquhar and Von Caemmerer (1982), Tenhunen *et al.* (1980), de Wit *et al.*

(1978) to simpler application oriented models such as those of Charles-Edwards and Ludwig (1974), Van Bavel (1975) and others summarized in Milthorpe and Moorby (1979).

The more detailed models explore the role of enzyme kinetics in the photosynthetic process and provide the researcher with insights regarding the limiting factors exerted by the environment (for example, PAR) and the plant's biochemistry (for example, the size of the ribulose diphosphate pool).

The simpler models, on the other hand, have a long history of field application and are relatively easy to fit to data. They generally take the form of

$$P_n = \frac{a_1 F\downarrow}{b_1 + F\downarrow} - R_d \tag{15}$$

where P_n is the photosynthetic rate (mg CO_2 m^{-2} s^{-1} or mg CO_2 dm^{-1} $hour^{-1}$), $F\downarrow$ is the normal (relative to leaf) flux density of incident visible radiation (PAR) (W m^{-2}), R_d is the dark respiration rate (mg CO_2 m^{-2} s^{-1}) and a_1 and b_1 are constants (mg CO_2 m^{-2} s^{-1} or mg CO_2 dm^{-1} $hour^{-1}$ and W m^{-2}, respectively).

The value of a_1 may be taken as the maximum gross photosynthetic rate for a saturating irradiance while the value of b_1 determines the gradient of the initial response of photosynthesis at low irradiances. The dark respiration rate R_d, has been variously described as a 'property tax', dependent on plant biomass, or as an 'income tax', dependent on the photosynthetic rate (see, for example, Angus and Wilson 1976); generally it may be assumed to be a relatively small fraction of gross photosynthesis.

Equation (15) can be made to fit observations reasonably well (see, for example, Zelitch 1971) and will be used to represent the net photosynthetic rate of an individual leaf in the following discussion.

3.2. *Leaf stomatal resistance*

The stomatal resistance of a leaf is the means by which a plant controls the gas exchange between the leaf interior and free atmosphere. Farquhar (1978), Farquhar *et al.* (1980), Farquhar and Sharkey (1982) and Williams (1983) have presented theoretical arguments and some evidence which support the thesis that stomatal functioning operates in such a way as to minimize the rate of water loss per unit photosynthate assimilated. The exchange of water vapour between the saturated air space within a leaf substomatal cavity and the external air may be written as

$$\lambda E = \frac{(e^*(T_c) - e_a)}{r_s + r_b} \frac{\rho c_p}{\gamma} \tag{16}$$

where λE is the latent heat flux (W m^{-2}), ρ and c_p are the density (kg m^{-3}), and specific heat of air (J kg^{-1} K^{-1}), respectively, γ is the psychrometric constant (mbar K^{-1}), $e^*(T_c)$ is the saturated vapour pressure at leaf temperature, T_c (mbar), e_a is the vapour pressure outside the leaf (mbar), r_s is the stomatal resistance (s m^{-1}) and r_b is the boundary layer resistance (s m^{-1}). (r_s may be thought of as the inverse of the sum of all the diffusion conductances of individual stomata acting in parallel—usually $r_s > r_b$).

Jarvis (1976) analysed a large data set of r_s values obtained for two coniferous species and his expression for r_s as a function of environmental variables may be rearranged to give

$$r_s = \left[\frac{a_2}{b_2 + F\downarrow} + c_2\right] [f(\psi_l) f(T_c) f(e_a)]^{-1} \tag{17}$$

where a_2, b_2 and c_2 are constants (J m^{-3}, W m^{-2} and s m^{-2}, respectively) and $f(\psi_l)$,

$f(T_c)$ and $f(e_a)$ are the adjustment factors for the influence of leaf water potential, ψ_l, leaf temperature, T_c, and vapour pressure, e_a. The factors are limited to the range 0–1. The constants a_2, b_2 and c_2 may be fitted to measurements of r_s (see, for example, Gee and Federer 1972, Fletcher 1976, Tan and Black 1978, Kaufmann 1976). For this study, data from Turner (1974) were used to obtain the parameters a_2, b_2 and c_2 for a maize leaf, see table 1. If one accepts the arguments favouring a constant ratio between P_n and the transpiration rate, it is relatively easy to derive values of a_2, b_2 and c_2 from a consideration of the constants in the photosynthetic equation, equation (15), the constant of water-use efficiency and an assumed climatic mean evaporative demand. For the present, however, the values of the constants in equation (17) are determined from fitting to data. The form of the adjustment factors are described in full in Jarvis (1976) but will not be reviewed here; most of the following analysis assumes near optimal conditions for both photosynthesis, as given by equation (15), and stomatal functioning, as given by the first term in parentheses in equation (17).

3.3. *Simplification of the description of the attenuation of photosynthetically active radiation in plant canopies*

Equations (15) and (17) are adequate descriptions of processes on an isolated leaf. In order to estimate the area-averaged photosynthetic rate and canopy resistance (resistance to vapour transfer imposed by the canopy per unit ground area) we must integrate these expressions over all the leaves in the canopy.

Before doing this, we must make some simple assumptions about the way PAR is attenuated, absorbed and utilized within a canopy. Direct beam radiation incident on a canopy of randomly distributed elements with near-zero scattering coefficients will be attenuated in accordance with the exponential extinction law of Monsi and Saeki (1953)

$$I_L = I_0 \exp(-KL) \tag{18}$$

where I_0 is the incident radiation above canopy (W m^{-2}) and I_L is the radiation below a leaf-area index of L (W m^{-2}).

The attenuation of radiation when the scattering coefficient is non-zero has been already discussed in the previous section. For small values of ω ($\omega \leqslant 0{\cdot}2$, for PAR), however, Goudriaan (1977) found that equation (18) could be modified to give good numerical values of the intensity profile by a simple empirical adjustment of the extinction coefficient:

$$F_L = F_0 \exp(-kL); \qquad k = [G(\mu)/\mu](1-\omega)^{1/2} \tag{19}$$

It is normal practice to estimate the photosynthetic rate and resistance of whole canopies by considering the separate contributions made by leaves exposed to full (direct beam) sunlight and shade leaves (see, for example, Isobe 1967, Sinclair *et al.* 1976, Jahnke and Lawrence 1965). The areas of sunlit and shade leaves are calculated by using equation (18)

$$\begin{aligned} \text{sunlit area} &= [1-\exp(-KL_T)]/K \\ \text{shaded area} &= L_T - [1-\exp(-KL_T)/K \end{aligned} \tag{20}$$

It seems more reasonable, however, to assume that the photosynthetic rate and the total resistance of an ensemble of leaves of similar orientation and position in the canopy will be closer to estimates obtained by using *one* mean irradiance (as calculated

from equation (19) rather than summing the two components represented by equation (20)). The arguments one can put forward for this are:

(1) Leaves of the same orientation at the canopy top will all be sunlit while those at the canopy base will be receiving mainly scattered light.
(2) Leaf position changes with the wind and the Sun moves during the day and so sunflecks cannot be assumed to stay focused on an individual leaf inside the canopy long enough for it to attain a steady-state photosynthetic rate and stomatal aperture. Ino (1969, 1970) reported that the radiative flux density beneath a sugar-beet canopy showed three to six peaks per 10 s. Woods and Turner (1971) reported that the time constant for the stomatal function of four deciduous tree species was of the order of 3–20 min for opening stomata and 12–35 min for closing stomata. If, as Williams (1983) observed, stomata remain in a slightly 'too open' state (in terms of water-use efficiency), the longer time constant appropriate to the closing response will be applicable.
(3) If, the real situation were closer to that represented by equation (20) rather than by equation (19), we would expect canopies to consist of large flat regularly spaced leaves, nearly all of which would be sunlit, with little radiation penetrating below a leaf-area index of 1. While this arrangement is broadly true of shade-loving species, which have to make the best use of low radiation incomes, it does not seem to hold for most upper storey vegetation (see, for example, Goudriaan 1977, Parkhurst and Loucks 1972, Davis and Taylor 1980).

3.4. *Canopy photosynthesis and resistance*

Equations (15) for leaf photosynthesis, (17) for leaf stomatal resistance and (19) for radiation attenuation may now be combined to estimate integral values of photosynthesis and stomatal resistance for whole canopies. In doing this, we must assume that most of the absorbed PAR is intercepted in the direction of the incident beam—obviously this will be in error when considering processes at the canopy base but the results indicate that this effect is not serious.

Leaves will differ in their photosynthetic rates and stomatal resistance values according to

(1) the strength of the incident PAR flux, and therefore the position of the leaf in the canopy,
(2) the orientation of the leaves to the PAR flux, and
(3) the preconditioning of the leaf: leaves at the top of the canopy (sun leaves) tend to exhibit higher maximum photosynthetic rates and lower minimum stomatal resistance values than the 'shade' leaves at the canopy base (see, for example, Alderfer 1975).

With regard to the last point, it is not thought that the variations in leaf properties will greatly affect the validity of this analysis. Most data indicate that leaves within a canopy exhibit roughly the same initial responses to incident PAR flux at low irradiances. The transition from the semilinear relationship between photosynthesis and irradiance over to the asymptotic light-saturated condition occurs over a relatively narrow irradiance interval and at decreasing values of irradiance deeper within the canopy. Now under normal illumination conditions, the leaves deeper in the canopy are operating below their light-saturated limits (due to the effects of shading) and so

their actual performance may be described by the low irradiance section of the sun leaves' response.

If we assume that all the leaves in the canopy react to incident PAR as defined by equation (15), the photosynthetic rate of the whole canopy may be written as

$$P_c = \int_0^{L_T} \int_0^{\pi/2} \int_0^{2\pi} P_n(F, \xi, \theta) O(\xi, \theta) \sin\theta \, d\xi \, d\theta \, dL \tag{21}$$

where P_c is the photosynthetic rate of the whole canopy, (mg CO_2 m^{-2} s^{-1}), $O(\xi, \theta)$ is the leaf-angle distribution function and ξ and θ are azimuth and inclination angles, respectively.

Table 3 gives the solutions obtained for equation (21) for a few leaf-angle distribution functions with the dark respiration term, R_d, omitted. When using the Ross (1975) χ_L function, the angular integrals are omitted as the function gives a *mean*

Table 3. Canopy photosynthetic rate, P_c, as a function of leaf-area index, L_T, the leaf-angle distribution function and PAR flux above the Canopy, F_0. All other symbols are defined in text. (Direct PAR only.)

Horizontal leaves

$$P_c = \frac{a_1}{k} \ln\left(\frac{b_1 + F_0}{b_1 + F_0 \exp(-kL_T)}\right)$$

Spherically distributed leaves

$$P_c = a_1 L_T + \frac{a_1 b_1 \mu}{k F_0} \{g_1 - g_2 - g_3\}$$

$$g_1 = \exp(kL_T) \ln\left(\frac{\mu b_1}{\mu b_1 + F_0 \exp(-kL_T)}\right)$$

$$g_2 = \ln\left(\frac{\mu b_1}{\mu b_1 + F_0}\right)$$

$$g_3 = \frac{F_0}{\mu b_1} \ln\left(\frac{\mu b_1 \exp(kL_T) + F_0}{\mu b_1 + F_0}\right)$$

Vertical leaves

$$P_c = a_1 L_T - \frac{2a_1}{\pi k} M_{\phi_0}^{\phi L_T}$$

$$\phi > 1,\ M = \sum_{i=0}^{\infty} \frac{E_{2i} y^{2+2i}}{(2+2i)2i!},\ y = 2\tan^{-1}\sqrt{\left(\frac{\phi - 1}{\phi + 1}\right)},\ E = \text{Euler number}$$

$$\phi < 1,\ M = \ln(1+\phi) - 2\sum_{j=2}^{\infty} \frac{1}{j}\left(\frac{\phi - 1}{\phi + 1}\right)^j \sum_{n=2}^{j} \frac{(-1)}{2n-1)}$$

$$\phi = \beta \exp(kL),\ \beta = \frac{\mu b_1}{F_0(1-\mu^2)^{1/2}}$$

Ross–Goudriaan function: $G(\mu) = \phi_1 + \phi_2 \mu$

$$P_c = \frac{a_1}{k} \ln\left[\frac{\mu b_1 + G(\mu) F_0}{\mu b_1 + G(\mu) F_0 \exp(-kL_T)}\right]$$

projection in the direction μ so that equation (21) becomes

$$P_c = \int_0^{L_T} P_n(F, G(\mu))\, dL \tag{22}$$

where $G(\mu)$ is the mean projection of leaves in direction μ.

Equation (22) represents a simplification of equation (21) in using the mean leaf projection to calculate the activity of all the leaves (see, for example, Monsi 1968) at a given depth in the canopy while equation (21) takes the effect of the distribution of leaf orientations into account explicitly. Numerically, however, equations (21) and (22) give similar results for the same leaf-angle distributions. This finding, and calculations of P_c and canopy resistance, r_c, for diffuse radiation indicate that the vegetation's response is relatively insensitive to the direction of incoming radiation (except for vertical and near-vertical leaves) over the middle range of solar angles.

If we assume, as before, that leaves at all levels in the canopy react in a similar way to incident PAR, the bulk canopy resistance, r_c, may be written as

$$\frac{1}{r_c} = \int_0^{L_T} \int_0^{\pi/2} \int_0^{2\pi} \frac{O(\xi, \theta)}{r_s(F, \xi, \theta)} \sin\theta\, d\xi\, d\theta\, dL \tag{23}$$

Table 4 lists solutions to equation (23). A solution for the Ross–Goudriaan χ_L function (Goudriaan 1977) (equivalent to equation (22) for P_c) is also given.

3.5. *Comparison of predicted and observed canopy photosynthesis*

There have been few experimental studies where leaf and canopy photosynthesis were measured simultaneously. Figure 10 shows the net photosynthetic response of an individual wheat leaf as observed by Evans and Dunstone (1970) with some individual data points for net photosynthesis from Denmead (1976) for comparison. Using values of a_1 and b_1 fitted to the data of Evans and Dunstone (1970), P_c was calculated for whole wheat canopies with leaf-area indices of 1·6 and 3·2 for clear days in January, i.e. the Australian summer, via equation (21). We have assumed that R_d is a constant fraction of gross photosynthesis in this instance which may produce errors at low irradiances. The PAR was assumed to be half of the incident global radiation in both cases.

These calculations are plotted against the corresponding data in figure 10. Two features are immediately apparent, first, additional increments of leaf-area index are predicted to yield diminishing returns in terms of the total net photosynthetic rate and, secondly, the response of a whole canopy is more linear than that of an individual leaf held normal to the same flux. The first effect is due to the shading of leaves at the base of the canopy. The cause of the second effect is to be found in the way the incident flux is partitioned in the canopy; spherically distributed leaves will maintain the same distribution of leaf inclinations relative to the incoming beam regardless of the solar elevation, but the path length will decrease from a maximum at low solar elevations to a minimum for an overhead Sun. The combination of these two phenomena—shading and the interaction of leaf inclination and solar elevation—tends to linearize the response of P_c to global radiation.

3.6. *Comparison of predicted and observed canopy resistance values*

As with photosynthesis, few studies of stomatal resistance have correlated processes at the level of a leaf with the functioning of an entire canopy. First, we should question the validity of using the integral of all the leaf stomatal resistance values as an

Table 4. Canopy resistance, r_c, as a function of leaf-area index, L_T, the leaf-angle distribution function and PAR flux above the canopy, F_0. All other symbols are defined in text. (Direct PAR only.)

Horizontal leaves

$$\frac{1}{r_c}=\frac{1}{kc_2}\left[\frac{b_2}{dF_0}\ln\left(\frac{d\exp(kL_T)+1}{d+1}\right)-\ln\left(\frac{d+\exp(-kL_T)}{d+1}\right)\right]$$

$$d=\frac{a_2+b_2c_2}{c_2F_0}$$

Spherically distributed leaves

$$\frac{1}{r_c}=\frac{1}{kc_2}\left[kL_T-\frac{a_2\mu}{c_2F_0}(g_4-g_5+g_6)\right]$$

$$g_4=\exp(kL_T)\ln\left(1+\frac{1}{\Omega\exp(kL_T)}\right)$$

$$g_5=\ln(1+1/\Omega)$$

$$g_6=\frac{1}{\Omega}\ln\left(\frac{\Omega\exp(kL_T)+1}{\Omega+1}\right),\ \Omega=d\mu$$

Vertical leaves

$$\frac{1}{r_c}=\frac{L_T}{c_2}-\frac{2}{\pi k}\frac{a_2}{(a_2+b_2c_2)c_2}M_{\phi_0}^{\phi L_T}$$

M = as defined in table 3

$$\phi=\beta\exp(kL),\ \beta=\frac{\mu d}{(1-\mu^2)^{1/2}}$$

Ross-Goudriaan function: $G(\mu)=\phi_1+\phi_2\mu$

$$\frac{1}{r_c}=\frac{1}{kc_2}\left[\frac{b_2}{dF_0}\ln\left\{\frac{\mu d\exp kL_T+G(\mu)}{\mu d+G(\mu)}\right\}-\ln\left\{\frac{\mu d+G(\mu)\exp(-kL_T)}{\mu d+G(\mu)}\right\}\right]$$

approximation to the canopy resistance term used in 'unilayer' models of evapotranspiration (see, for example, Monteith 1973).

Tan and Black (1976) used a numerical analogue of equation (23) to estimate canopy resistance for a Douglas Fir stand in British Columbia, Canada. Their results indicated that the omission of terms representing the different gradients of T_c, e_a and T_a in the canopy did not greatly affect the estimation of the canopy transpiration rate implying that r_c as given by (23) should provide us with a usable estimate of evapotranspiration when inserted in the Penman–Monteith equation (see, for example, Monteith 1973), providing the soil surface and canopy are dry. Monteith *et al.* (1965) measured the stomatal resistance of barley leaves with a viscous flow porometer and estimated the surface resistance of the crop as a residual of an energy-balance calculation. Figure 11 shows a comparison of the results of Monteith *et al.* (1965) and the estimate of r_c as given by equation (23) for spherically distributed leaves using values of a_2, b_2 and c_2 fitted to the porometer data of r_s for an individual leaf. Both the trend and magnitude of the predicted surface resistance are in reasonable agreement with the observations. The divergence between the observed and calculated

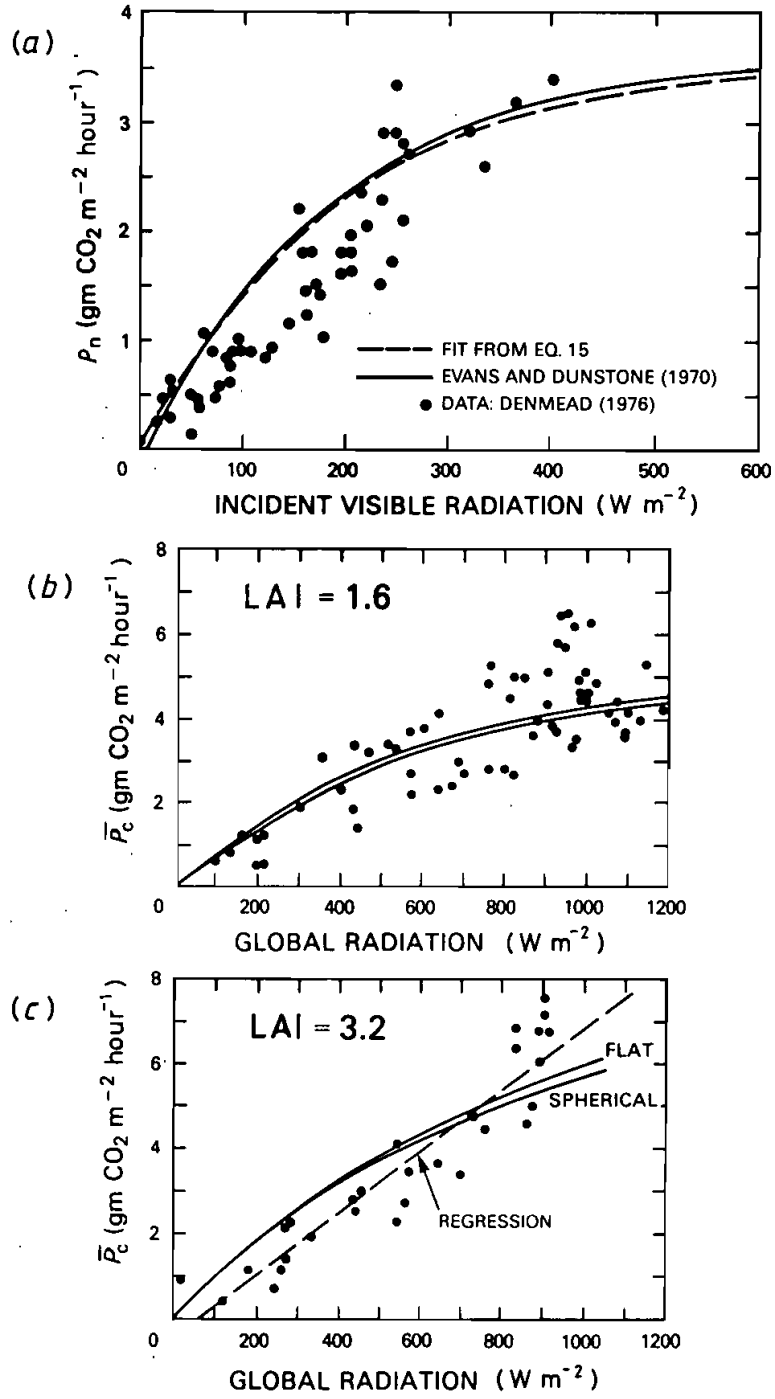

Figure 10. (*a*) Relation between net photosynthetic rate of individual wheat leaves and incident visible radiation. Solid line is from Evans and Dunstone (1970), dashed line is best fit of equation (15) in text, points are for another wheat crop (see Denmead 1976). (*b*) and (*c*) show the calculated net photosynthetic rates (from equation (21) and dashed line in (*a*)) of whole wheat canopies for two leaf area indices and two leaf-angle distributions compared with measurements of Denmead (1976).

values of r_c at high radiation incomes may be attributed to the effects of leaf water potential on stomatal closure at high transpiration rates.

Figure 12 shows the variation of r_c with leaf-area index as measured by Monteith *et al.* (1965) and as predicted by equation (23). For the predictions, daily mean values of r_c were obtained by assuming clear days on the appropriate dates and totally green

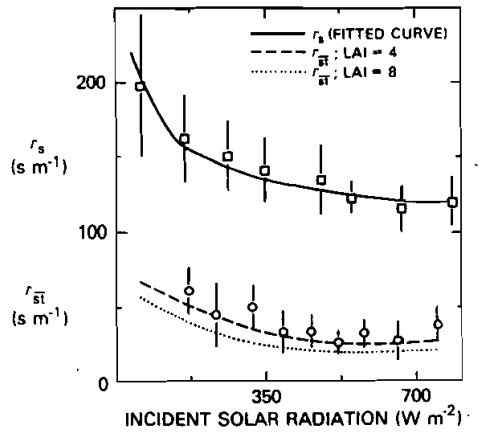

Figure 11. Relation between leaf stomatal resistance (r_s) and irradiance for individual barley leaves. Open squares are data from Monteith *et al.* (1965), vertical lines are error bars, solid line is best fit of equation (17) in text. Lower part of figure shows estimated surface resistance for a barley crop (open circles) from Monteith *et al.* (1965) compared with values of the canopy resistance, r_{st}, as given by equation (23) for two leaf-area indices.

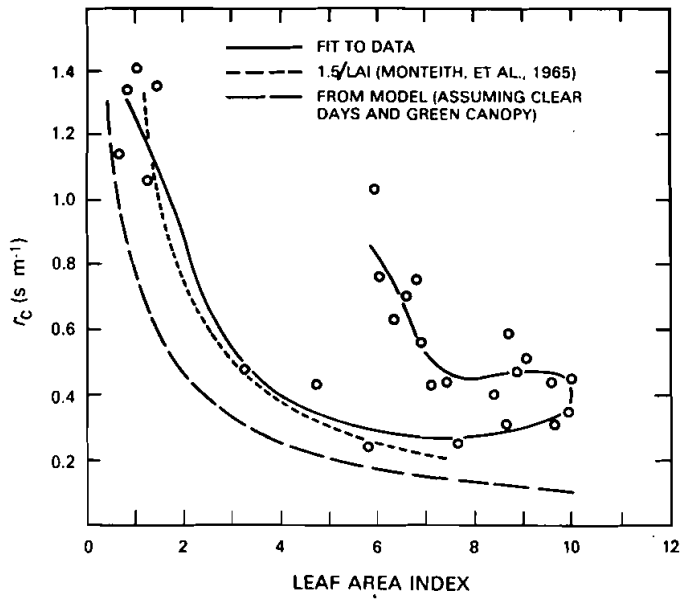

Figure 12. Observed (open circles and solid line) course of surface resistance of a barley crop over a growing season. Also shown is the suggested relationship as proposed by Monteith *et al.* (1965) and value of minimum canopy resistance as calculated from equation (23) in the text.

canopies. We expect the predictions to undershoot the observations by a slight amount during the growing phase (due to less than clear conditions) and to significantly underestimate r_c as the crop senesces. Both trends are apparent in figure 12.

Some confirmation of the predicted variation in r_s with canopy position may be obtained from the data of Watts *et al.* (1976). Watts *et al.* (1976) measured profiles of r_s in a Sitka spruce canopy and the results qualitatively concur with the combination of equation (19) with equation (23). Canopy resistance was calculated numerically from the profiles in the same way as Tan and Black (1976) and the results emphasize the dominance of the upper layers of the canopy in determining the transpiration rate.

3.7. *Diurnal variation of canopy photosynthesis and resistance*

Figures 13 and 14 show the predicted variation of P_c and r_c with leaf-area index, the angle of incoming radiation and leaf orientation. Clearly, a saturation effect occurs at the higher leaf-area indices, which is increased if the cover or greenness fraction is reduced (see later discussion). In all cases, the coefficients used in calculating r_c and P_c were fitted to data for maize (see table 1).

Most of the above discussion has been concerned with instantaneous values of P_c and r_c. We shall now consider daily mean estimates of these quantities which may be compared with observations taken intermittently during a growing season. Figure 15 shows time-averaged values of P_c and r_c for Julian day 180 at a latitude of 30°N. (Clear skies are assumed and Goudriaan's (1977) data relating visible and near-infrared radiation fluxes to the solar angle are used.) In all cases, P_c and r_c were obtained numerically by

$$\overline{P_c} = \frac{1}{M-D}\int_D^M P_c\,dt \tag{24}$$

$$\frac{1}{\overline{r_c}} = \frac{1}{M-D}\int_D^M \frac{1}{r_c}\,dt \tag{25}$$

$\overline{P_c}$ is the daily mean photosynthetic rate (mg CO_2 dm^{-1} $hour^{-1}$), $\overline{r_c}$ is the daily mean canopy resistance (s m^{-1}), D is the time of dawn and M is the time of midday.

3.8. *Relationships between absorbed photosynthetically active radiation and primary productivity*

The results shown in figure 13 may be compared with some field studies. Monteith (1977) presented results which indicate that net photosynthesis or growth could be related to the integrated amount of PAR absorbed by a canopy

$$\overline{P_c} = \frac{1}{\Delta t}\int_0^{\Delta t} \varepsilon F_a\,dt \tag{26}$$

where ε is the efficiency of conversion of PAR to net photosynthesis (gm CO_2 J^{-1}) and F_a is the PAR absorbed by the canopy (W m^{-2}).

The PAR absorbed by the canopy, F_a, may be calculated for the direct fraction by

$$F_a = F_0\{(1-\alpha_v) - [I\downarrow_{L_T} + \exp(-KL_T)(1-\rho_s)\} \tag{27}$$

F_0 is the downward flux of PAR above the canopy (W m^{-2}) and α_v is the albedo of the surface in the PAR wavelength interval, from equation (11). Figures 16 and 17 show

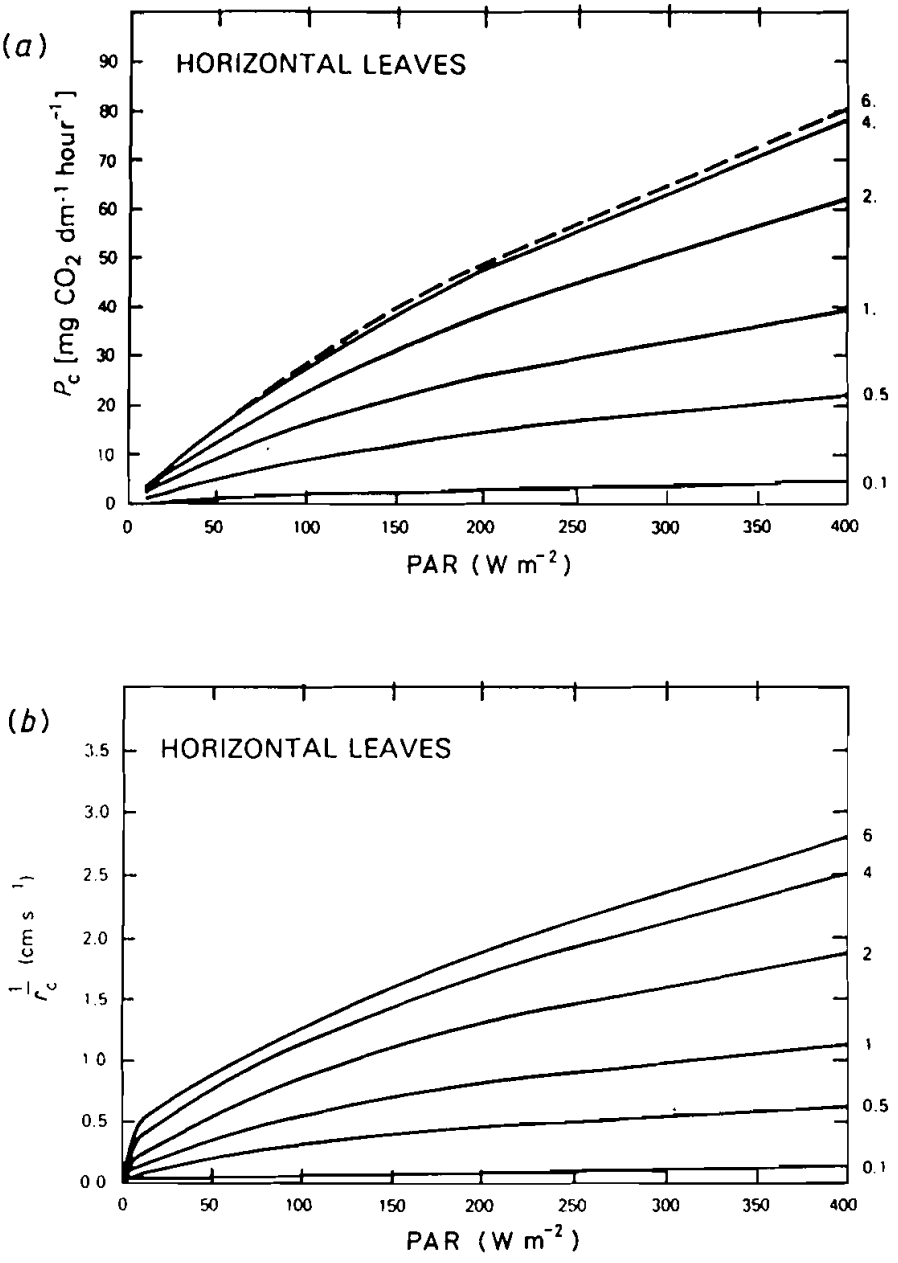

Figure 13. (*a*) Calculated canopy photosynthetic rate, P_c, as a function of leaf area index (numbers on the right-hand side of the figure) and incident PAR. P_c is given by equation (24) in the text using coefficients from table 1. Note diminishing effect of leaf area increments. The canopy is green and the solar elevation = 40°. (*b*) Calculated canopy resistance values, r_c, as a function of leaf area index (numbers on right-hand side of the figure) and incident PAR. r_c is given by equation (25) in the text. (Other conditions as in (*a*).)

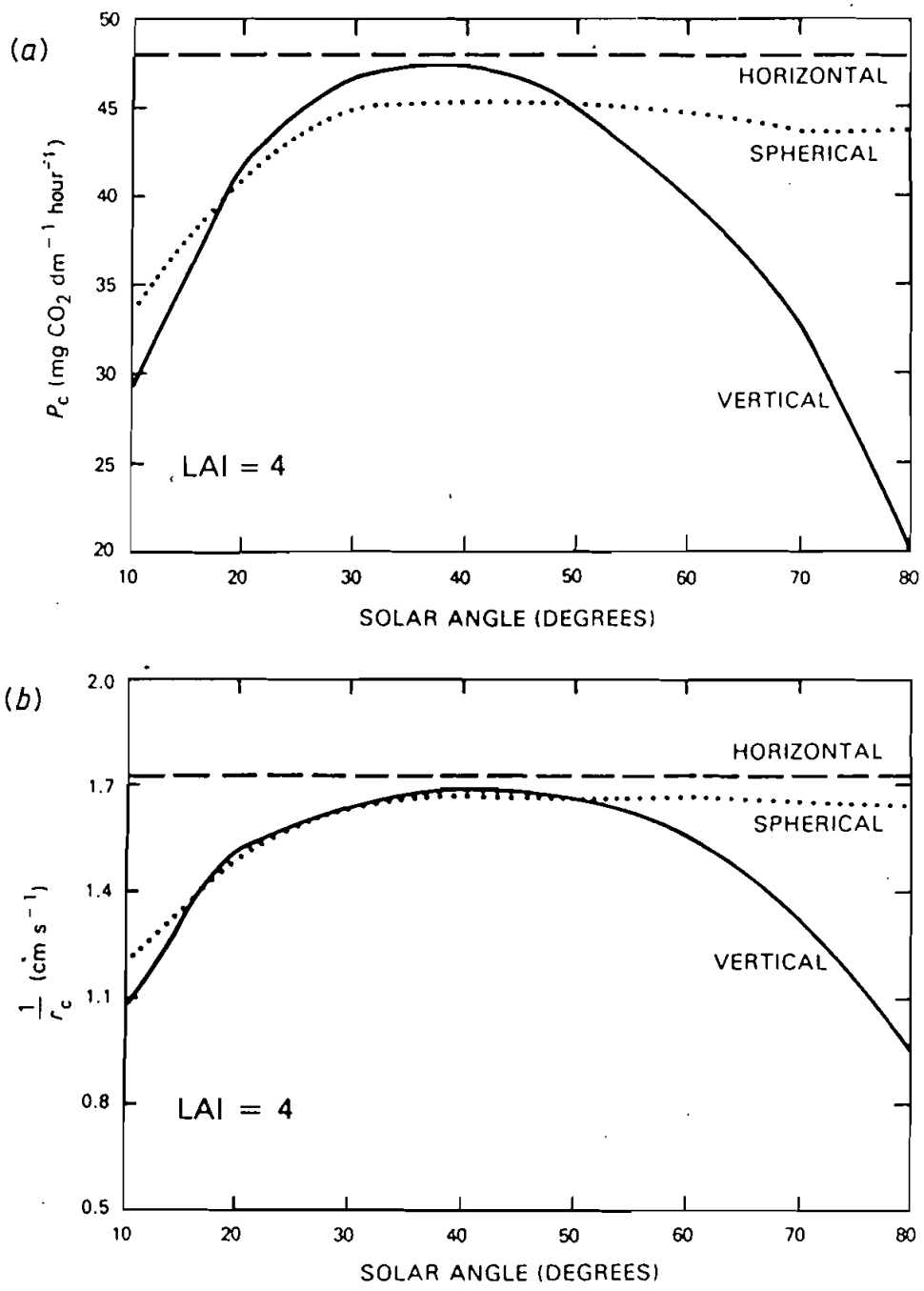

Figure 14. Calculated effect of solar elevation on (*a*) canopy photosynthetic rate, P_c, and (*b*) canopy resistance, r_c, for three leaf-angle inclinations. PAR = 200 W m^{-2} throughout, which yields no change in the photosynthetic response of horizontal leaves with solar angle.

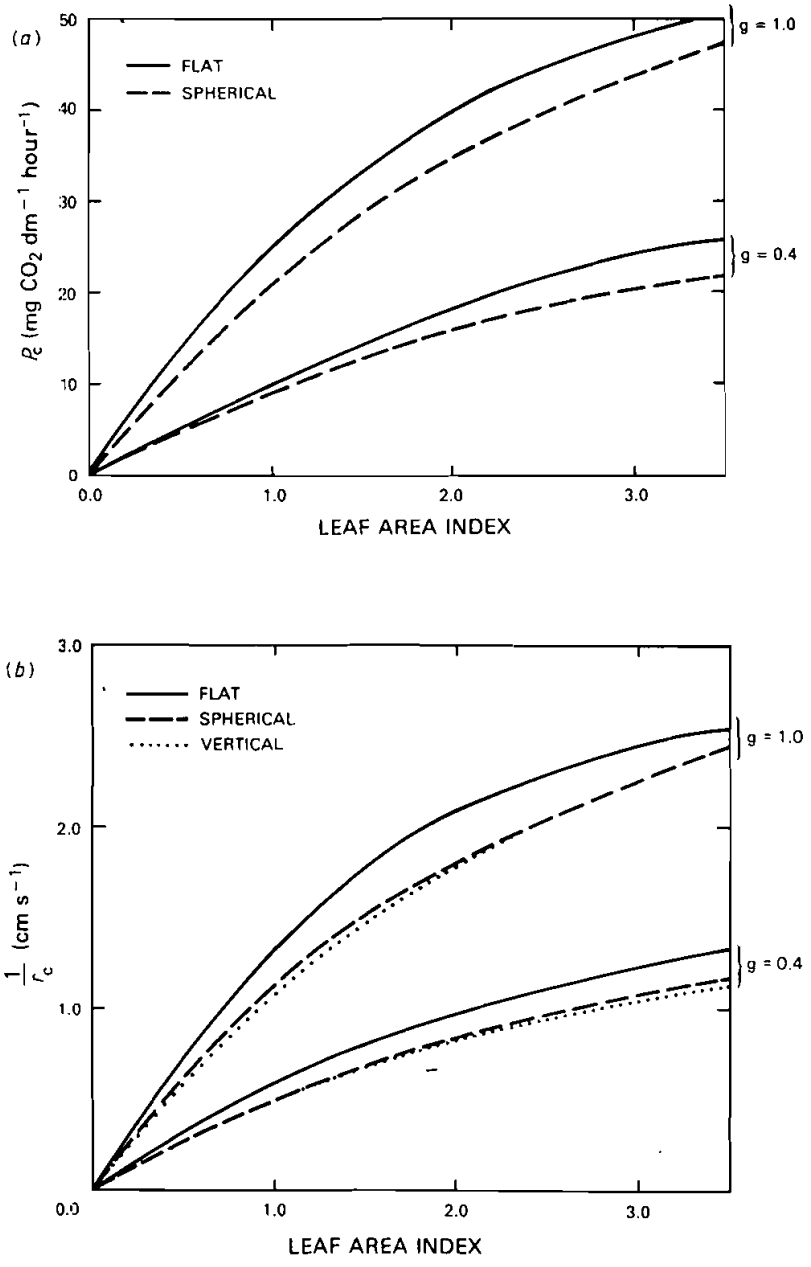

Figure 15. (*a*) Calculated relation between daily mean photosynthetic rate, $\overline{P_c}$, and leaf-area index for two leaf-angle distributions and two greenness values, 'g'. Values are for a maize canopy (table 1) on Julian day 180 at 30°N. (*b*) Calculated relation between daily mean canopy resistance, $\overline{r_c}$, and leaf-area index for two leaf-angle distributions and two greenness values, 'g'. Values are for a maize canopy (table 1) on Julian day 180 at 30°N.

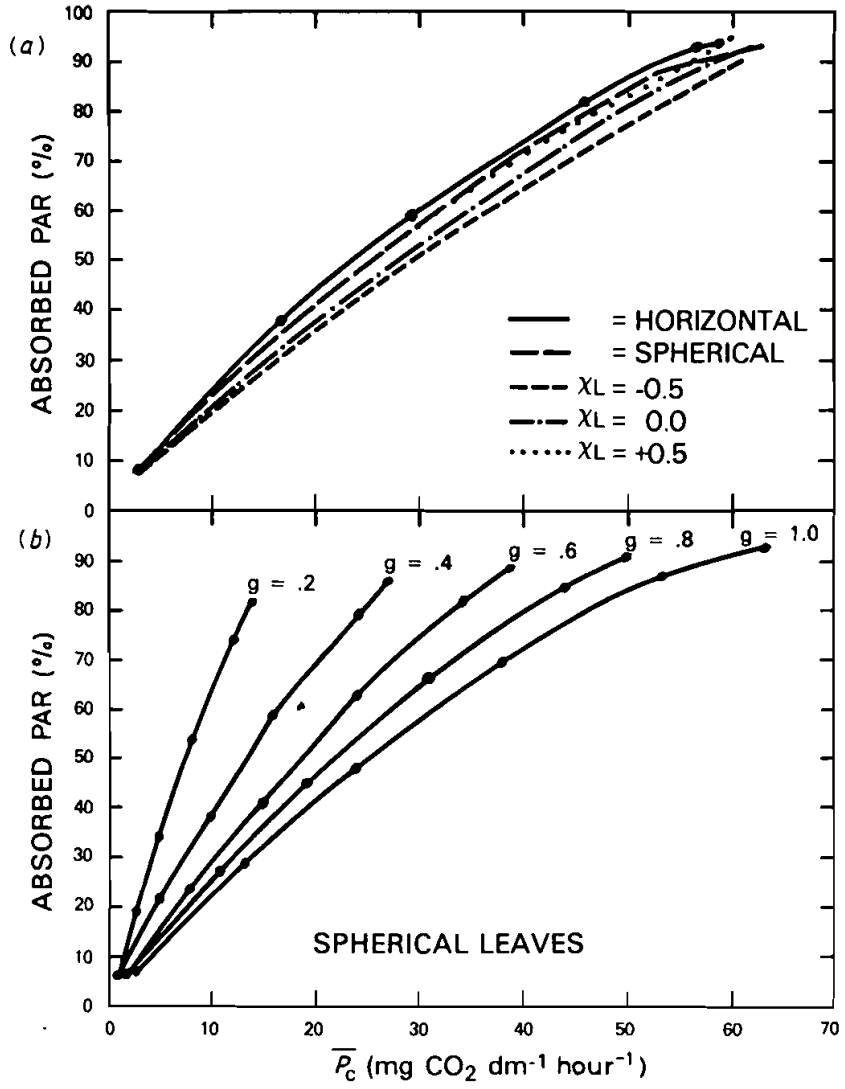

Figure 16. Calculated relation between $\overline{P_c}$ and absorbed fraction of PAR for (*a*) a range of leaf-angle distributions and (*b*) a range of canopy greenness values, 'g'. Solid circles on lines denote leaf area indices of 0·1, 0·5, 1·0, 2·0, 4·0 and 6·0, working from left to right on each line. Crop is maize (table 1) and values are calculated for Julian day 180 at 30°N.

the model estimates of the daily integral of F_a against $\overline{P_c}$ and $\overline{r_c}$. The relationship is predicted to be near linear for green vegetation, a result which is not intuitively obvious given the non-linear dependence of P_c on F. It is clear that the combination of two non-linear functions, one describing the attenuation of PAR, the other relating incident PAR to r_c and P_c, yields this result. The asymptotic behaviour of the two functions are mutually self-cancelling, a finding which implies that the stomatal response and canopy architecture are related in order to make the most efficient use of the incident radiation. A by-product of these relationships is that the effect of increasing leaf area

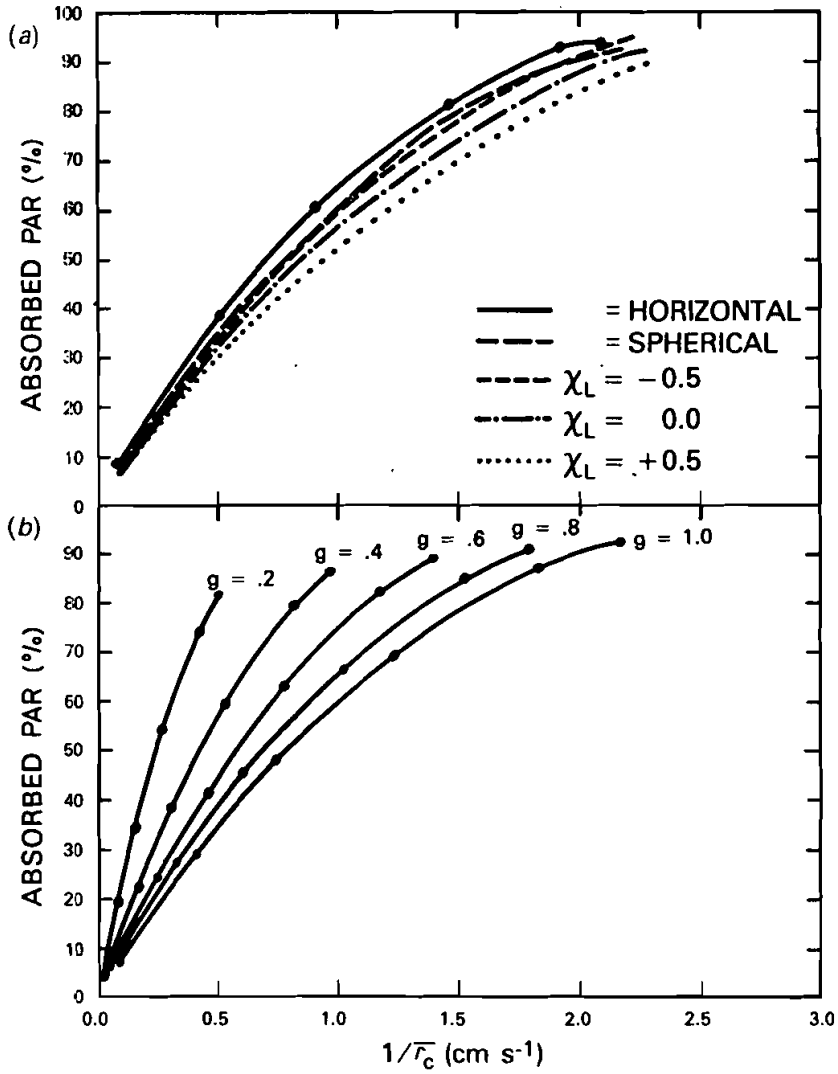

Figure 17. Calculated relation between $\overline{r_c}$ and absorbed fraction of PAR for (*a*) a range of leaf-angle distributions and (*b*) a range of canopy greenness values, 'g'. Solid circles on lines denote leaf area indices of 0·1, 0·5, 1·0, 2·0, 4·0 and 6·0, working from left to right on each line. Other variables are the same as in figure 16.

index on P_c is calculated to fall off in a near-geometric fashion. Equation (26) might therefore be expected to perform well in regions where the crop is not subject to environmental stress.

3.9. *Summary of the performance of the canopy photosynthesis and resistance models*

From the discussion in the preceding sections, the integration of formulae describing photosynthesis and stomatal resistance for individual leaves over the depth of whole canopies seem to provide us with reasonable area-averaged estimates of photosynthesis and surface resistance (if we neglect soil evaporation). Additionally,

the integrated expressions give rise to the following predictions which are supported by what data are available:

(1) Additional increments in leaf area index have a diminishing effect on canopy photosynthesis and resistance due to the effects of shading.
(2) The combination of shading, leaf orientation and solar angle tend to linearize the photosynthetic and stomatal response of whole canopies to incident PAR.
(3) The linearizing effect predicted in (2) results in the prediction of a near-linear relation between plant growth rate and canopy resistance (and hence transpiration loss) and absorbed PAR in accordance with observations.

The above relationships are not expected to hold when the crop is subjected to stress or when leaf properties change drastically throughout the depth of the canopy.

4. Canopy photosynthesis, resistance and spectral reflectivity

4.1. *Limitations of the modelling approach*

Prior to interrelating the results of the previous sections, a summary of the limitations of the theoretical approach seems in order:

(1) The radiative transfer model (equations (1) and (2)) is not consistent with the expression used for describing the attenuation of PAR down through the canopy in equation (19).
(2) Few scattering processes are isotropic.
(3) The expressions describing leaf photosynthesis and resistance are empirical summaries of complicated processes.
(4) The physiological processes are considered in isolation from factors other than PAR, i.e. the effects of temperature, leaf water potential, humidity and leaf age have not been addressed.
(5) Leaf properties are assumed to be constant within the canopy.

In spite of the above, we shall assume that the trends predicted by the simple models should be indicative of what happens in reality.

4.2. *Relating canopy photosynthesis and resistance to spectral reflectivity*

Figures 18 and 19 show the predicted canopy photosynthetic rate, P_c, and the resistance, r_c, as functions of leaf area index and incoming photosynthetically active radiation. The corresponding simple-ratio values are predicted to be near linearly related to P_c and $1/r_c$, the slope of the relationship depending on the incident radiation intensity. While the same trend is apparent in the vegetation index values (see right-hand sides of figures), this quantity is less linearly related to either P_c or $1/r_c$ than the simple ratio. This result, which recurs throughout the following discussion, is due to the more rapid increase in the denominator and decrease in the numerator in the expression for vegetation index in equation (14) as green leaf area increases. The vegetation index therefore exhibits a swifter relative response at low leaf area indices and a more rapid saturation than the simple ratio.

Figures 20 and 21 compare the daily mean values, $\overline{P_c}$ and $\overline{r_c}$, to the simple ratio and the vegetation index as given by equations (1), (2) and (14). It is clear that while the simple ratio and vegetation index are not very sensitive predictors of leaf area index, they are simulated to be good indicators of the canopy photosynthetic capacity and resistance. The reason for this effect is obvious; $\overline{P_c}$, $\overline{r_c}$ and the reflectances approach

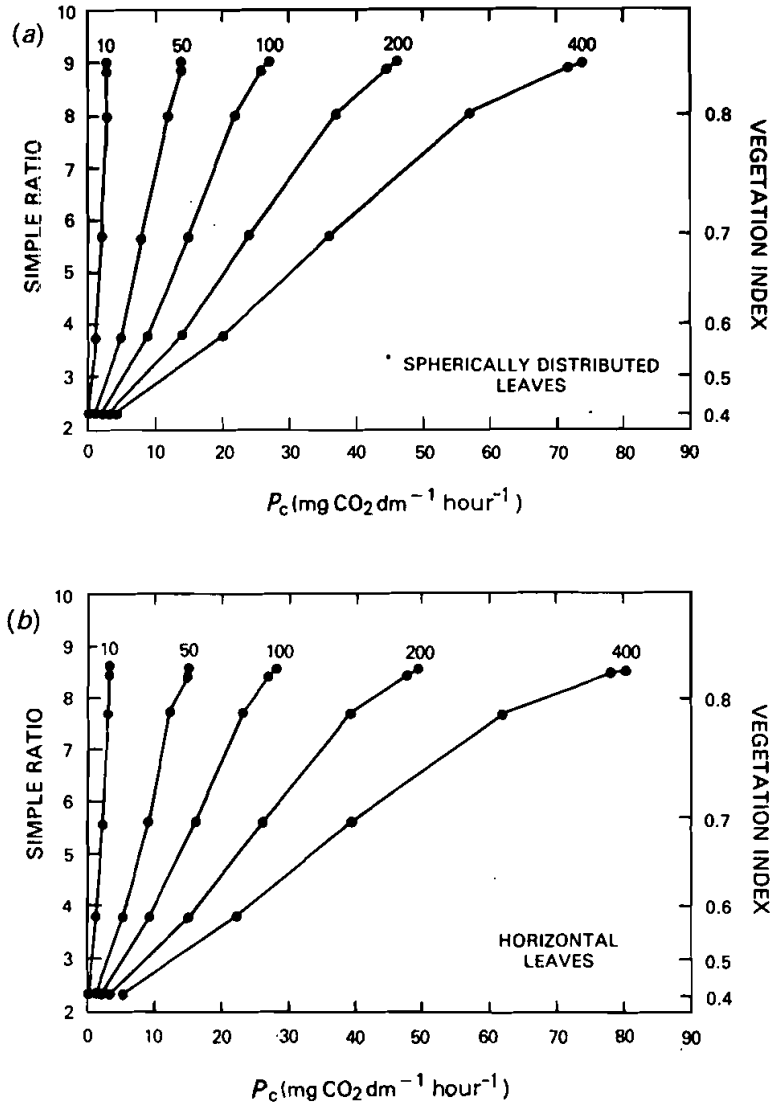

Figure 18. Calculated relation between the simple ratio/vegetation index, net photosynthetic rate, P_c, and incident PAR (numbers on graphs (W m^{-2})). Solid circles on the lines correspond to leaf area indices of 0·1, 0·5, 1·0, 2·0, 4·0 and 6·0, working from left to right. The crop is assumed to be a uniform green cover of maize (table 1) and the solar elevation is 30°.

asymptotes in a similar manner with increasing leaf area index. Daily averaged values of the vegetation index and simple ratio were obtained in a similar manner as $\overline{P_c}$ and $\overline{r_c}$. The near linearity of the relationship between $\overline{P_c}$ and the simple-ratio/vegetation-index estimates implies that a time integral of either of the latter quantities should be almost linearly related to the net or gross primary productivity of a canopy. The data of Goward *et al.* (1985) were summarized to produce a plot of the net primary productivity of a number of North American biomes against the time integral of the vegetation index over the growing season. These results show an almost linear

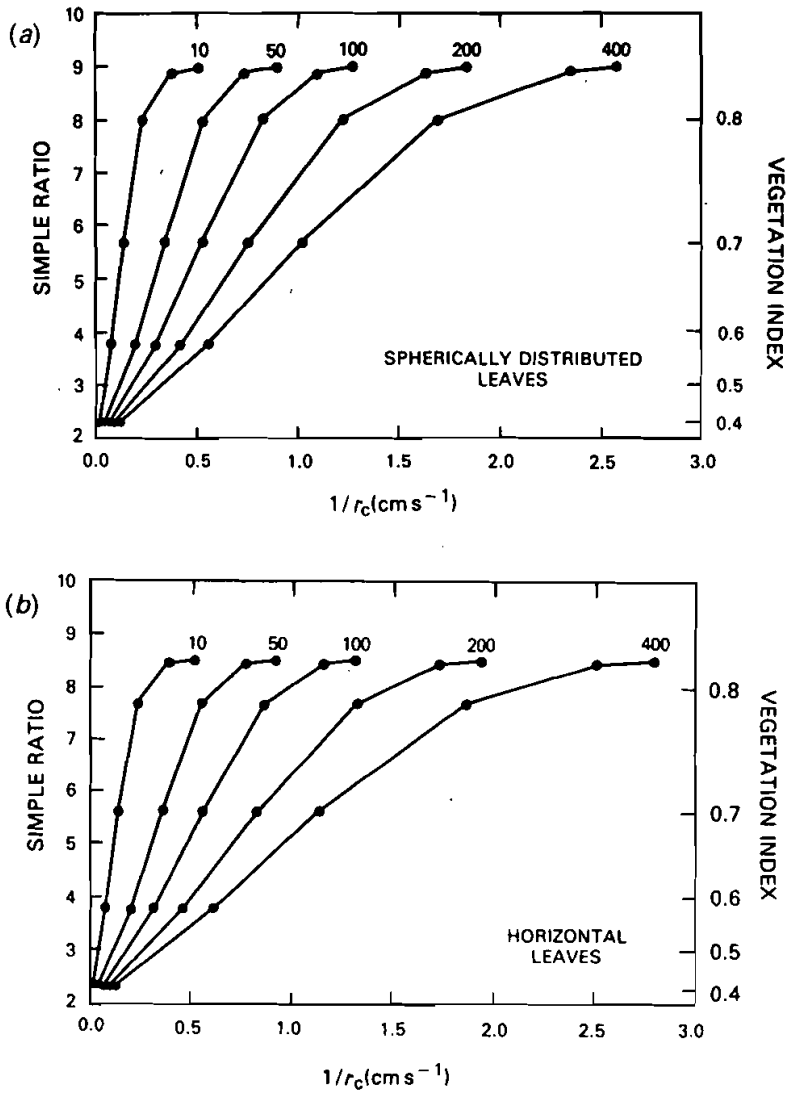

Figure 19. Calculated relation between the simple ratio/vegetation index, minimum canopy resistance, r_c, and incident PAR (numbers on graphs (W m^{-2})). Other variables are the same as in figure 18.

relationship between these two quantities in accordance with the calculations discussed above.

The above results indicate that although multispectral data may not be very useful in determining leaf area index, they may be able to provide usable estimates of the photosynthetic rate and canopy resistance, provided that other factors such as soil moisture, temperature, etc., are optimal and the incident flux of PAR is known. Accordingly, we may assign two functional attributes to a plant canopy on the basis of multispectral reflectance data. These are the photosynthetic capacity, P_c^*, and the canopy resistance function, r_c^*, which when combined with a given flux of PAR yield maximum values of P_c and $1/r_c$. Actual values of P_c and $1/r_c$ will drop below these

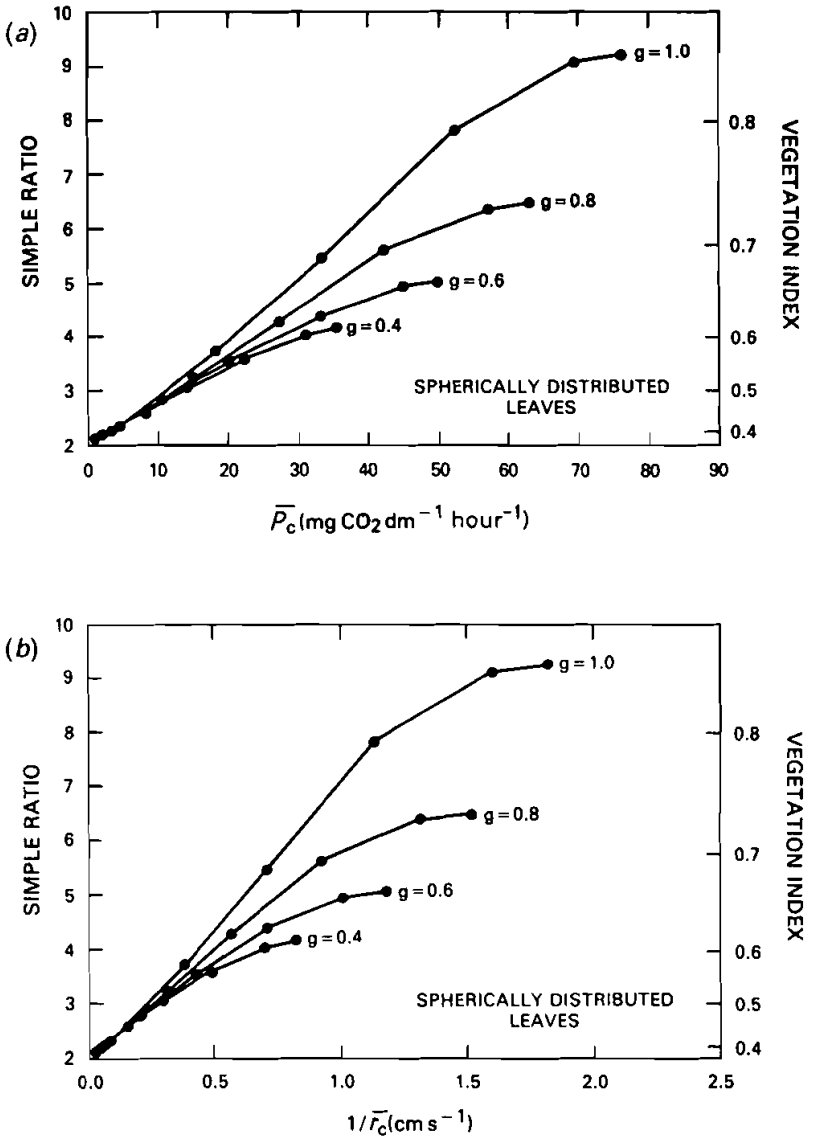

Figure 20. Calculated relation between the simple ratio/vegetation index (equation (14)) and (*a*) $\bar{P}_c$ and (*b*) $\bar{r}_c$. All variables and symbols are the same as in figures 18 and 19. Canopy has spherically distributed leaves. Variation with canopy greenness, denoted by 'g', is shown.

maxima if the canopy is subject to any kind of stress. A number of points should be borne in mind when considering these applications:

(1) Bare ground. The presence of even a small proportion of bare ground (as opposed to an even distribution of vegetation) may seriously complicate the interpretation of multispectral data. Figure 8 indicates that very dense vegetation confined to a 75 per cent cover would appear to correspond spectrally to a leaf-area index of just over unity for a continuous cover. (The

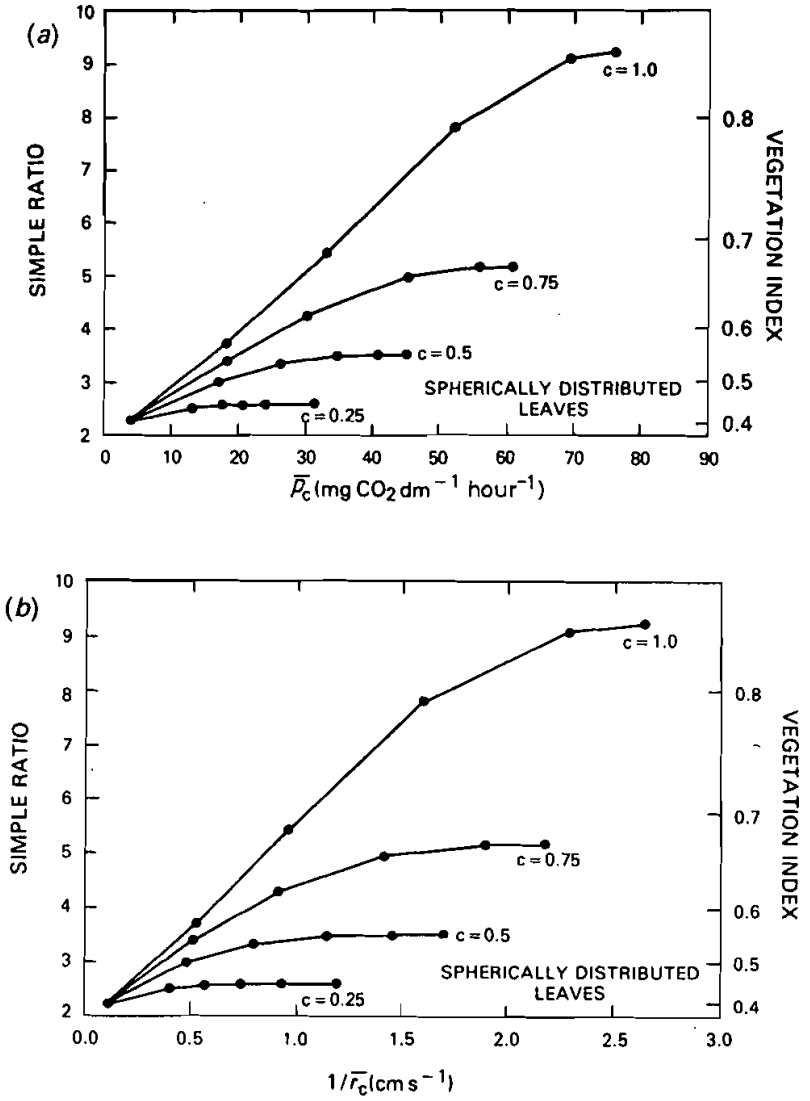

Figure 21. Calculated relation between simple ratio/vegetation index (equation (14)) and (*a*) $\overline{P_c}$ and (*b*) $\overline{r_c}$ for a green canopy with spherically distributed leaves for a range of cover fractions, denoted by 'c'. All other variables and symbols are the same as in figures 15 and 20.

figures will change, of course, with different values of soil reflectance, etc.) Figures 20 and 21 show that there is a corresponding uncertainty when relating $\overline{P_c}$ to the simple ratio.

(2) Greenness. The presence of even a small fraction of dead leaves in the canopy would appear to reduce the vegetation index and simple ratio drastically (see figures 20 and 21).

(3) Leaf orientation and solar elevation. The correlation of multispectral data with leaf area index is predicted to be significantly dependent on leaf orientation and solar elevation for leaves with angular distributions other than horizontal.

The effect increases in severity the more the leaves approach a vertical distribution. Such a result is not surprising in view of the fact that the single scattering albedo, $a_s(\mu)$, for vertical leaves varies from $\omega/2$ to zero as the solar elevation increases from zero to $\pi/2$.

(4) Viewing angle. Although not discussed here, operational measurements of surface reflectances are usually made with narrow field-of-view sensors. The relationship between the bidirectional reflectance and the biophysical quantities of P_c and r_c can be expected to vary with view angle, solar azimuth angle, etc. Here, only the integrated hemispherical reflectances are considered.

5. Conclusions

In conclusion, it would appear that multispectral data may be of some use in assessing the area-averaged biophysical activity of vegetation in a region as represented by the photosynthetic capacity, P_c^*, and the canopy resistance function, r_c^*. The assumed close relationship between these two quantities is supported by figure 22 where it appears that the functional relationship between leaf photosynthesis and transpiration rates translates to the analogous canopy terms for the maize data set used in this study. The problems posed by uncertainties in the cover fraction, leaf orientation, fraction of dead leaves and species mix (not addressed here) are considerable and it is clear from the results in the previous section that for the relationships between P_c, r_c and reflectance to be usable, either the vegetative cover must be continuous and green or further data concerning these factors must be available. High-resolution sensors operating in the visible and near-infrared channels may be applied to this problem.

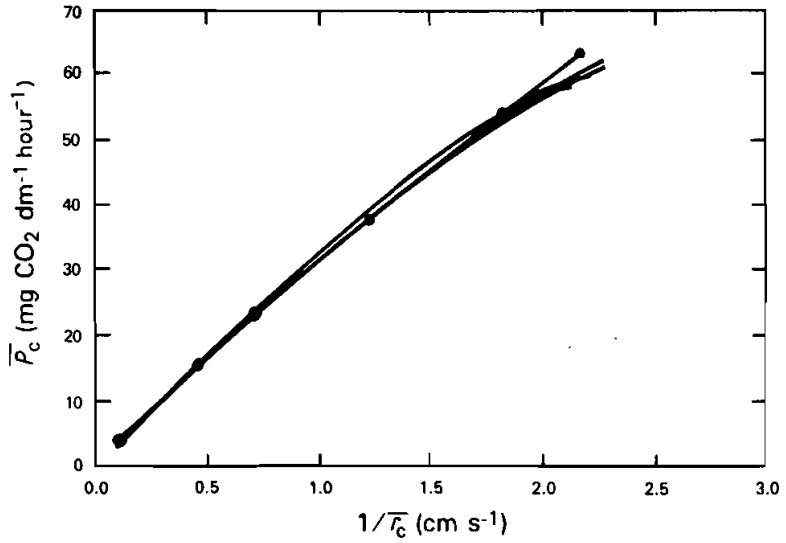

Figure 22. Calculated relation between $\overline{P_c}$ and $\overline{r_c}$ for a maize canopy (table 1), all other variables as before. The relations for five different leaf-angle distributions are shown but these are virtually indistinguishable from each other. Solid circles represent leaf-area indices of 0·1, 0·5, 1·0, 2·0, 4·0 and 6·0, working from left to right, origin represents leaf-area index of zero.

A major obstacle to using satellite observations of surface spectral reflectances in conjunction with physiological models is connected to the range of physiological responses exhibited by different species in a given plant community, all of which may be expected to contribute to the total area-averaged photosynthetic and transpiration rates in a complex and non-linear fashion. On the other hand, it is reasonable to assume that species occupying overlapping or adjacent niches (in ecological terms) will have similar physiognomies and physiological responses to environmental forcings (see, for example, Colinvaux 1973, Kormondy 1969, Dunn 1975, Taylor 1975). Obviously, this situation does not hold in many regions; for example, shrub–savanna consists of coexisting herbacious and shrubby vegetation with differing morphological and physiological characteristics (Walter, 1973) which implies that there are two broad groups of evolutionary stable strategies (see, for example, Dawkins 1976) for the vegetation under these particular climatic conditions. However, in other regions (tropical rain forest, grasslands, seasonal forests), the dominant species exhibit similarities in form and primary production rates. Here, the assumption of area-averaged canopy characteristics is not so unreasonable.

As mentioned before, this paper is exploratory and further work must be done with more sophisticated models in conjunction with field experiments to test the validity of the various assumptions made in the preceding analysis. It does seem, however, that some canopies may utilize the absorbed photosynthetically active radiation in a near-linear fashion and that the visible and near-infrared albedos may respond accordingly. That the simple ratio or vegetation index are poor predictors of leaf area index and biomass should not be surprising, therefore, but the indications that they may be able to provide more profound information regarding photosynthesis and transpiration are encouraging.

Acknowledgments

At the time of this work, Piers Sellers was a National Academy of Science/National Research Council Resident Research Associate. Special thanks for help with the integration of some of the formulae in this paper must be extended to A. Dalcher, P. J. Camillo, R. E. Dickinson and A. T. C. Chang. Helpful discussions with C. J. Tucker, B. J. Choudhury, G. Asrar, J. Norman, J. Monteith, R. J. Gurney, T. J. Schmugge, D. S. Kimes, B. N. Holben, S. N. Goward, Y. Kaufman and R. S. Fraser contributed to the final form of the paper. The impetus for the work was provided by R. E. Murphy and S. I. Rasool who while attending a workshop on the use of vegetation-index values simultaneously said "but what does it all mean?" Joyce Tippett is to be specially thanked for typing and editing the manuscript.

Appendix

Solution to two-stream approximation equations as described in the text.

Direct beam radiation

$$\left.\begin{aligned} I\uparrow &= \frac{h_1 \exp(-KL)}{\sigma} + h_2 \exp(-hL) + h_3 \exp(hL) \\ I\downarrow &= \frac{h_4 \exp(-KL)}{\sigma} + h_5 \exp(-hL) + h_6 \exp(hL) \end{aligned}\right\} \tag{10}$$

$$b = (1-(1-\beta)\omega)$$

$$c=\omega\beta$$
$$d=\omega\bar{\mu}K\beta_0$$
$$f=\omega\bar{\mu}K(1-\beta_0)$$
$$h=(b^2-c^2)^{1/2}/\bar{\mu}$$
$$\sigma=(\bar{\mu}K)^2+c^2-b^2$$
$$h_1=-dp_4-cf$$
$$h_2=\frac{1}{D_1}\left[\left(d-\frac{h_1}{\sigma}p_3\right)(u_1-\bar{\mu}h)\frac{1}{S_1}-p_2\left(d-c-\frac{h_1}{\sigma}(u_1+\bar{\mu}K)\right)S_2\right]$$
$$h_3=-\frac{1}{D_1}\left[\left(d-\frac{h_1}{\sigma}p_3\right)(u_1+\bar{\mu}h)S_1-p_1\left(d-c-\frac{h_1}{\sigma}(u_1+\bar{\mu}K)\right)S_2\right]$$
$$h_4=fp_3-cd$$
$$h_5=-\frac{1}{D_2}\left[\frac{h_4}{\sigma}(u_2+\bar{\mu}h)\frac{1}{S_1}+\left(u_3-\frac{h_4}{\sigma}(u_2-\bar{\mu}K)\right)S_2\right]$$
$$h_6=\frac{1}{D_2}\left[\frac{h_4}{\sigma}(u_2-\bar{\mu}h)S_1+\left(u_3-\frac{h_4}{\sigma}(u_2-\bar{\mu}K)\right)S_2\right]$$
$$u_1=b-c/\rho_s$$
$$u_2=b-c\rho_s$$
$$u_3=f+c\rho_s$$
$$S_1=\exp(-hL_T)$$
$$S_2=\exp(-KL_T)$$
$$p_1=b+\bar{\mu}h$$
$$p_2=b-\bar{\mu}h$$
$$p_3=b+\bar{\mu}K$$
$$p_4=b-\bar{\mu}K$$
$$D_1=p_1(u_1-\bar{\mu}h)\frac{1}{S_1}-p_2(u_1+\bar{\mu}h)S_1$$
$$D_2=(u_2+\bar{\mu}h)\frac{1}{S_1}-(u_2-\bar{\mu}h)S_1$$

Diffuse radiation

$$\left.\begin{aligned}I\uparrow&=h_7\exp(-hL)+h_8\exp(hL)\\ I\downarrow&=h_9\exp(-hL)+h_{10}\exp(hL)\end{aligned}\right\}$$
$$h_7=\frac{c}{D_1}(u_1-\bar{\mu}h)\frac{1}{S_1}$$
$$h_8=\frac{-c}{D_1}(u_1+\bar{\mu}h)S_1$$
$$h_9=\frac{1}{D_2}(u_2+\bar{\mu}h)\frac{1}{S_1}$$
$$h_{10}=\frac{-1}{D_2}(u_2-\bar{\mu}h)S_1$$

References

ALDERFER, R. G., 1975, Photosynthesis in developing plant canopies. In *Perspectives of Biophysical Ecology*, edited by D. M. Gates and R. B. Schmerl (New York: Springer-Verlag), pp. 227–238.

ANGUS, J. F., and WILSON, J. H., 1976, Photosynthesis of barley and wheat leaves in relation to canopy models. *Photosynthetica*, **10**, 367.

ASRAR, G., FUCHS, M., KANEMASU, E. T., and HATFIELD, J. L., 1984, Estimating absorbed photosynthetic radiation and leaf area index from spectral reflectance in wheat. *Agron. J.*, **76**, 300.

CHARLES-EDWARDS, D. A., and LUDWIG, L. J., 1974, A model for leaf photosynthesis by C_3 plant species. *Ann. Bot.*, **38**, 921.

COLINVAUX, P. A., 1973, *Introduction to Ecology* (New York: Wiley).

CURRAN, P. J., 1980, Multispectral photographic remote sensing of vegetation amount and productivity. *Proceedings of the 14th International Symposium on Remote Sensing of the Environment*, Ann Arbor, Michigan, pp. 623–637.

DAVIS, J. M., and TAYLOR, S. E., 1980, Leaf physiognomy and climate: a multivariate analysis. *Quaternary Res.*, **14**, 337–348.

DAWKINS, R., 1976, The Selfish Gene (Oxford: Oxford University Press).

DENMEAD, O. T., 1976, Temperate cereals. In *Vegetation and the Atmosphere II*, edited by J. L. Monteith (New York, London: Academic Press), pp. 1–31.

DE WIT, C. T., *et al.*, 1978, *Simulation of Assimilation, Respiration and Transpiration of Crops*, (New York: Wiley).

DICKINSON, R. E., 1983, Land surface processes and climate-surface albedos and energy balance. *Adv. Geophys.*, **25**, 305.

DUNN, E. L., 1975, Environmental stresses and inherent limitations affecting CO_2 exchange in evergreen sclerophylls in Mediterranean climates. In *Perspectives of Biophysical Ecology*, edited by D. M. Gates and R. B. Schmerl (New York: Springer-Verlag), pp. 159–181.

EVANS, L. T., and DUNSTONE, R. L., 1970, Some physiological aspects of evolution in wheat. *Aust. J. biol. Sci.*, **23**, 725.

FARQUHAR, G. D., 1978, Feedforward responses of stomata to humidity. *Aust. J. Pl. Physiol.*, **5**, 487.

FARQUHAR, G. D., and SHARKEY, T. D., 1982, Stomatal conductance and photosynthesis. *An. Rev. Pl. Physiol.*, **33**, 317.

FARQUHAR, G. D., and VON CAEMERRER, S., 1982, Modeling of photosynthetic response to environmental conditions. In *Encyclopedia of Plant Physiology*, Vol. 12B, edited by O. L. Lange, P. S. Noble, C. B. Osmond and H. Ziegler (Berlin; Heidelberg: Springer-Verlag), pp. 549–558.

FARQUHAR, G. D., VON CAEMERRER, S., and BERRY, J. A., 1980, A biochemical model of photosynthetic CO_2 assimilation in leaves of C_3 species. *Planta (Berl.)*, **149**, 78.

FLETCHER, N., 1976, Patterns of leaf resistance to lodgepole pine transpiration in Wyoming. *Ecology*, **57**, 339.

FUCHS, M., ASRAR, G., KANEMASU, E. T., and HIPPS, L. E., 1983, Leaf area estimates from measurements of photosynthetically active radiation in wheat canopies. NASA Technical Report SR-M3-04420, NASA/JSC, ERRD, Houston, 77058, U.S.A.

GEE, G. W., and FEDERER, C. A., 1972, Stomatal resistance during senescence of hardwood leaves, *Wat. Resour. Res.*, **8**, 1456.

GOUDRIAAN, J., 1977, *Crop Micrometeorology: A Simulation Study*. (Wageningen; Wageningen Center for Agricultural Publishing and Documentation).

GOWARD, S. N., TUCKER, C. J., and DYE, D. G., 1985, North American vegetation patterns observed with the NOAA-7 Advanced Very High Resolution Radiometer, *Vegetatio* (in the press).

HESKETH, J. D., and BARKER, D., 1967, Light and carbon assimilation by plant communities. *Crop Sci.*, **7**, 285.

INO, Y., 1969, CO_2 fixation activity of cut leaf under intermittent illumination conditions. JIBP/PP-Photosynthesis Level III Experiments 1968, pp. 56–59. From *Photosynthesis and Productivity in Different Environments*, edited by J. P. Cooper (London: Cambridge University Press), pp. 301–302.

INO, Y., 1970, The effect of fluctuating light on photosynthesis. JIBP/PP-Photosynthesis Level III Experiments 1969, pp. 68–70. [ibid.]

ISOBE, S., 1967, Theory of light distribution and photosynthesis in canopies of randomly dispersed foliage area. *Bull. Nat. Inst. Sci.* A, **16,** 1.

JAHNKE, L. S., and LAWRENCE, D. B., 1965, Influence of photosynthetic crown structure on potential productivity of vegetation based primarily on mathematical models. *Ecology*, **46,** 319.

JARVIS, P. G., 1976, The interpretation of the variations in leaf water potential and stomatal conductance found in canopies in the field. *Phil. Trans. R. Soc.* B, **273,** 593.

KAUFMANN, M. R., 1976, Stomatal response of Engelmann spruce to humidity, light and water stress. *Plant Physiol.*, **57,** *898.*

KIMES, D. S., 1984, Modeling the directional reflectance from complete homogeneous vegetation canopies with various leaf orientation distributions. *J. opt. Soc. Am.* A, **1,** 725.

KORMONDY, E. J., 1969, *Concepts of Ecology*. (Englewood Cliffs, New Jersey: Prentice-Hall).

MEADOR, W. E., and WEAVER, W. R., 1980, Two-stream approximations to radiative transfer in planetary atmospheres: a unified description of existing methods and a new improvement. *J. atmos. Sci.*, **37,** 630.

MILLER, L. D., 1972, Passive remote sensing of natural resources. Dept. Watershed Science, Colorado State University, Colorado.

MILTHORPE, F. L., and MOORBY, J., 1979, *An Introduction to Crop Physiology*, 2nd edition (New York: Cambridge University Press).

MONSI, M., 1968, Mathematical models of plant communities. In *Functioning of Terrestrial Ecosystems at the Primary Production Level*, edited by E. F. Eckardt (Paris: UNESCO), pp. 131–149.

MONSI, M., and SAEKI, T., 1953, Uber den Lichtfactor in den Pflanzengesellschaft und seine Bedeutung fur die Stoffproduktion. *Jap. J. Bot.*, **14,** 22.

MONTEITH, J. L., 1973, *Principles of Environmental Physics*. (London: Edward Arnold).

MONTEITH, J. L., 1977, Climate and the efficiency of crop production in Britain. *Phil. Trans. R. Soc.* B, **281,** 277.

MONTEITH, J. L., SZEICZ, G., and WAGGONER, P. E., 1965, The measurement and control of stomatal resistance in the field. *J. appl. Ecol.*, **2,** 345.

NORMAN, J. M., and JARVIS, P. G., 1975, Photosynthesis in Sitka Spruce (*Picea Sitchensis* (Bong.) Carr.), V. *J. appl. Ecol.*, **839.**

PARKHURST, D. G., and LOUCKS, O. L., 1972, Optimal leaf size in relation to environment. *J. Ecol.* **60,** 505.

ROSS, J., 1975, Radiative transfer in plant communities. In *Vegetation and the Atmosphere*, Vol. 1, edited by J. L. Monteith (London: Academic Press), pp. 13–52.

SINCLAIR, T. R., MURPHY, C. E., and KNOERR, K. R., 1976, Development and evaluation of simplified models for simulating canopy photosynthesis and transpiration. *J. appl. Ecol.*, **13,** 813.

SUITS, G. H., 1972, The calculation of the directional reflectance of a vegetative canopy. *Remote Sensing Environ.*, **2,** 117.

TAN, C. S., and BLACK, T. A., 1976, Factors affecting the canopy resistance of a Douglas-Fir forest. *Boundary-Layer Met.*, **10,** 475.

TAN, C. S., and BLACK, T. A., 1978, Evaluation of a ventilated diffusion porometer for the measurement of stomatal diffusion resistance of Douglas-Fir needles. *Arch. Met. Geophys. Bioklim.* B, **26,** 257.

TAYLOR, S. E., 1975, Optimal leaf form. In *Perspectives of Biophysical Ecology*, edited by D. M. Gates and R. B. Schmerl (New York: Springer-Verlag), pp. 73–86.

TENHUNEN, J. D., HESKETH, J. D., and GATES, D. M., 1980, Leaf photosynthesis models. In *Predicting Photosynthesis for Ecosystem Models*, Vol. II, edited by J. D. Hesketh and J. W. Jones. (CRC Press), (Boca Raton: CRC Press), pp. 17–47.

TUCKER, C. J., HOLBEN, B. N., ELGIN, J. H., and MCMURTREY, 1981, Remote sensing of total dry matter accumulation in winter wheat. *Remote Sensing Environ.*, **11,** 171.

TURNER, N. C., 1974, Stomatal response to light and water under field conditions. *R. Soc. N.Z. Bull.*, **12,** 423.

VAN BAVEL, C. H. M., 1975, A behavioral equation for leaf carbon dioxide assimilation and a test of its validity. *Photosynthesis*, **9,** 165.

VAN DER PLOEG, R. R., TASSONE, G., and VON HOYNINGEN-HEUNE, J., 1980, The joint measuring campaign 1979 in Ruthe (West Germany)—description of Preliminary Data. E.E.C. Joint Research Center, Ispra.

WALTER, H., 1973, *Vegetation of the Earth: In Relation to Climate and Eco-physiological Conditions* (New York, Heidelberg, Berlin: Springer-Verlag), pp. 238.

WATTS, W. R., NEILSON, R. E., and JARVIS, P. G., 1976, Photosynthesis in Sitka Spruce (*Picea Sitchensis* (Bong.) Carr.)), VII. *J. appl. Ecol.*, **13**, 623.

WILLIAMS, W. E., 1983, Optimal water-use efficiency in a California shrub. *Plant, Cell Environ.*, **6**, 145.

WOODS, D. B., and TURNER, N. C., 1971, Stomatal response to changing light by four tree species of varying shade tolerance. *New Phytol.*, **70**, 77.

ZELITCH, I., 1971, *Photosynthesis, Photorespiration and Plant Productivity* (New York: Academic Press).